Geol. Mag. **146** (*4*), *2009, pp. 465–484. © 2009 Cambridge University Press*
doi:10.1017/S0016756809006268 *Printed in the United Kingdom*

New carbon isotope stratigraphy of the Ediacaran–Cambrian boundary interval from SW China: implications for global correlation

DA LI*, HONG-FEI LING*†, SHAO-YONG JIANG*, JIA-YONG PAN*‡, YONG-QUAN CHEN*, YUAN-FENG CAI* & HONG-ZHEN FENG*

*State Key Laboratory for Mineral Deposits Research, Department of Earth Sciences, Nanjing University, Nanjing 210093, China
‡Resource and Environmental Engineering Center, East China Institute of Technology, Fuzhou 344000, China

(*Received* 30 August 2007; *revised version received* 30 August 2008; *accepted* 28 October 2008; First published online 26 March 2009)

Abstract – The Yangtze Platform preserves relatively thick carbonate successions and excellent fossil records across the Ediacaran–Cambrian boundary interval. The intensely studied Meishucun section in East Yunnan was one of the Global Stratotype Section candidates for the Precambrian–Cambrian boundary. However, depositional breaks were suspected in the section and the first appearance of small shelly fossils could not be verified. The Laolin section located in NE Yunnan is more continuous and shows great potential for global correlation of carbon isotope features across the Precambrian–Cambrian boundary. However, the stratigraphic framework and correlations were controversial. We studied and systematically sampled the Laolin section and present here new carbon isotope data for this section. The Laolin section consists of, in ascending order, the Baiyanshao dolostone of the Dengying Formation, the Daibu siliceous dolostone, Zhongyicun dolomitic phosphorite, lower Dahai dolostone and upper Dahai limestone of the Zhujiaqing Formation, and the black siltstone of the Shiyantou Formation. Our data reveal a large negative $\delta^{13}C$ excursion (−7.2 ‰, L1′) in the Daibu Member, which matches the previously published data for the Laolin section, and a large positive excursion (+3.5 ‰, L4) in the Dahai Member, which was not shown in the published data. The excursion L1′ correlates well with the similarly large negative excursion near the first appearance of small shelly fossils in Siberia and Mongolia. Similar magnitude excursions are also known from Morocco and Oman, for which there are no robust fossil constraints but from where volcanic ash beds have been dated precisely at 542 Ma, thus confirming a global biogeochemical event near the Ediacaran–Cambrian boundary. Our data also indicate that deposition was more continuous at the Laolin section compared with the Meishucun section, where there are no records of a comparable negative excursion near the Ediacaran–Cambrian boundary, nor any comparable positive excursion in the Dahai Member. Therefore, the Laolin section has proven potential to be a supplementary Global Stratotype Section for the Ediacaran–Cambrian boundary on the Yangtze Platform.

Keywords: C-isotope stratigraphy, Ediacaran–Cambrian boundary, Laolin section, Yangtze Platform.

1. Introduction

The Precambrian–Cambrian (Ediacaran–Cambrian) boundary was defined at the first appearance (FAD) of trace fossils called *Phycodes pedum* (Narbonne *et al.* 1987; Brasier, Cowie & Taylor, 1994) or *Trichophycus pedum* (Geyer & Uchman, 1995) at Fortune Head, southeastern Newfoundland, Canada. As this Global Stratotype Section and Point of the Ediacaran–Cambrian boundary was established mainly on the basis of trace fossils in siliciclastic strata, the wider correlation of shallow marine carbonate strata with this stratotype has been difficult in practice. Fortunately, carbon isotope stratigraphy has shown great potential to be a powerful complement to biostratigraphy for global correlation of Ediacaran–Cambrian successions (e.g. Kaufman & Knoll, 1995; Brasier *et al.* 1996). The Yangtze Platform in SW China crops out in well-preserved and carbonate-dominated sections across the Ediacaran–Cambrian boundary, which may provide good opportunity to elucidate C-isotope evolution over the Ediacaran–Cambrian boundary interval. The most continuous successions across the Ediacaran–Cambrian boundary on the Yangtze Platform are found in eastern Yunnan Province (Luo *et al.* 1980; Qian *et al.* 1996; Zhu *et al.* 2001, 2003). Studies on lithology, biostratigraphy and chemostratigraphy have been carried out for the famous Meishucun section (Qian, 1977; Luo *et al.* 1980, 1982, 1984, 1990; Brasier *et al.* 1990). However, the level of the FAD of small shelly fossils there is controversial (Jiang, 1980; Luo *et al.* 1982; Qian & Bengtson, 1989; Qian *et al.* 1996), and the expected negative C-isotope excursion near the supposed Ediacaran–Cambrian boundary seen in many other places in the world was not observed (Brasier *et al.* 1990).

Recently, Shen & Schidlowski (2000) observed a few negative and positive C-isotope excursions across the Ediacaran–Cambrian boundary at the potentially more complete Laolin section in NE Yunnan and

†Author for correspondence: hfling@nju.edu.cn

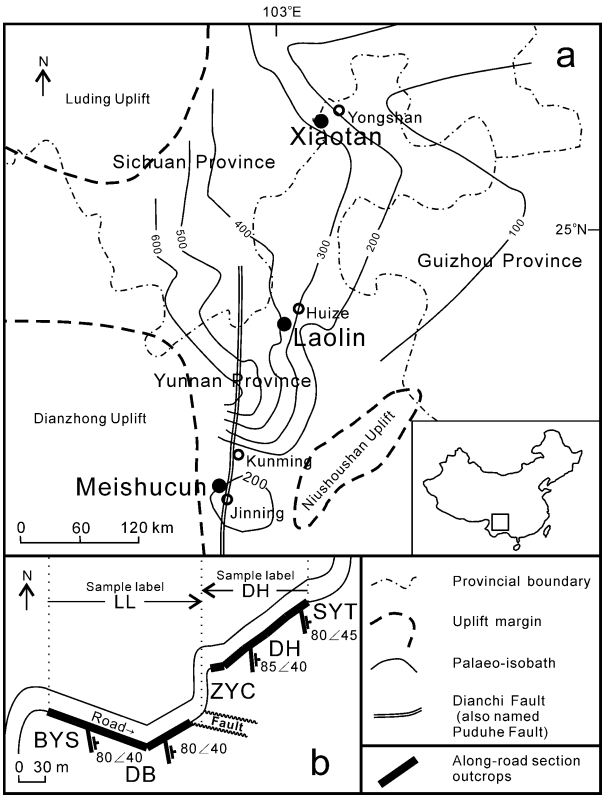

Figure 1. (a) Palaeogeographic and schematic geographic map showing localities of Laolin, Meishucun and Xiaotan sections in NE Yunnan, SW China; (b) schematic stretch of Laolin section, showing the sampled places along the road with geological member divisions, dip direction and dip angle. BYS – Baiyanshao Member; DB – Daibu Member; ZYC – Zhongyicun Member; DH – Dahai Member; SYT – Shiyantou Formation.

placed the Ediacaran–Cambrian boundary at Marker A near the bottom of the 'Xiaowaitoushan Member'. However, their stratigraphic framework, the placement of the Ediacaran–Cambrian boundary, and implied global correlations were doubted by Zhu, Li & Zhang (2001). Zhu and his colleagues also suspected that the Dahai Member was not completely sampled by Shen & Schidlowski (2000), as their $\delta^{13}C$ values are all below zero, whereas peak $\delta^{13}C$ values from the Dahai Member at the Meishucun section are above +1 ‰ (Brasier *et al.* 1990). It was considered necessary to restudy the section for two main reasons: (1) the sedimentary units of the earliest Cambrian in the region east of the Dianchi Fault (including the Laolin section) are thicker and hence probably more continuous than those found west of the fault (where the Meishucun section is situated) (Qian *et al.* 1996) (Fig. 1a; see below for details); (2) negative and positive C-isotope excursions have been reported from the Laolin section (Shen & Schidlowski, 2000), but both stratigraphic details and correlations are disputed (e.g. Zhu, Li & Zhang, 2001) and clearly need refinement. For the present study, we systematically sampled the Laolin section and analysed carbonate C-isotope compositions in order better to constrain C-isotope trends across the Ediacaran–Cambrian boundary and in so doing achieve better correlation with other regions of the world.

2. Stratigraphic features and previous work

2.a. Stratigraphic comparison with Meishucun section

The sedimentary records from the terminal Neoproterozoic to early Cambrian in Huize County of NE Yunnan Province where the studied Laolin section (Luo, Wu & Ouyang, 1991) is located, and in Kunming area where the well-known Meishucun section (e.g. Qian, 1977; Luo *et al.* 1980; Cowie, 1985; Qian & Bengtson, 1989) is located, are similar, although differences have been revealed (Qian *et al.* 1996; Zhu *et al.* 2001) which are stated below and illustrated in Figure 2.

To compare the sections, we summarize the stratigraphic features of the Meishucun section first. According to Luo *et al.* (1980, 1982, 1984, 1990) and Luo, Wu & Ouyang (1991), the Meishucun section consists in upward succession of the 'Xiaowaitoushan Member', Zhongyicun Member, Dahai Member, Badaowan Member (later renamed as Shiyantou Member) (Figs 2, 3). The 'Xiaowaitoushan Member', having a thickness of 7.4 m, comprises intermediate (0.1–0.5 m) to thick (0.5–2 m) beds of light grey silty dolostone intercalated with some black chert plates or flat lenses, and in the uppermost part with some phosphorite beds (Luo *et al.* 1980). The chert plates or lenses appear discontinuously in a horizontal direction (He, 1989). Luo *et al.* (1980) claimed that this member contained small shelly fossils of *Anabarites*, *Turcutheca*, *Circotheca*, *Hyolithellus*, *Cassidina* and *Artimycta*, whose FAD was named Marker A. However, as the 'Xiaowaitoushan Member' and the underlying Baiyanshao Member are lithologically identical, Luo and his colleagues have been changing the placement of the base of the 'Xiaowaitoushan Member' in concordance with revisions of the position of the first occurrence of small shelly fossils, from 4.2 m to 7.4 m (Luo *et al.* 1982) or 8.2 m (Xing *et al.* 1984) below the base of the phosphorite of the overlying Zhongyicun Member. This clearly indicates that the 'Xiaowaitoushan Member' as originally defined was a biostratigraphic rather than a lithostratigraphic unit. From a lithostratigraphic viewpoint and from the observation that the FAD of small shelly fossils in the 'Xiaowaitoushan Member' could not be verified, the 'Xiaowaitoushan Member' was interpreted to be part of the Baiyanshao Member of the upper Dengying Formation (He, Shen & Yin, 1988; He, 1989; Qian & Bengtson, 1989; Qian *et al.* 1996; Qian, 1999). Integrated evidence shows an erosion surface on top of the Xiaowaitoushan Member which is overlain by the Zhongyicun Member (Fig. 2). The lithology and sedimentary facies changed suddenly from the intertidal–supratidal silty dolostone of the 'Xiaowaitoushan Member' to subtidal algae bank phosphorite of the Zhongyicun Member (Qian *et al.* 1996). Deposition of the 'Xiaowaitoushan Member' and the underlying Baiyanshao Member was within a single continuous marine facies of regressive systems tract, while deposition of the Zhongyicun Member switched abruptly to relatively high-energy environments (He, 1989; Qian *et al.* 1996). The vertical variation of the

https://doi.org/10.1017/S0016756809006268 Published online by Cambridge University Press

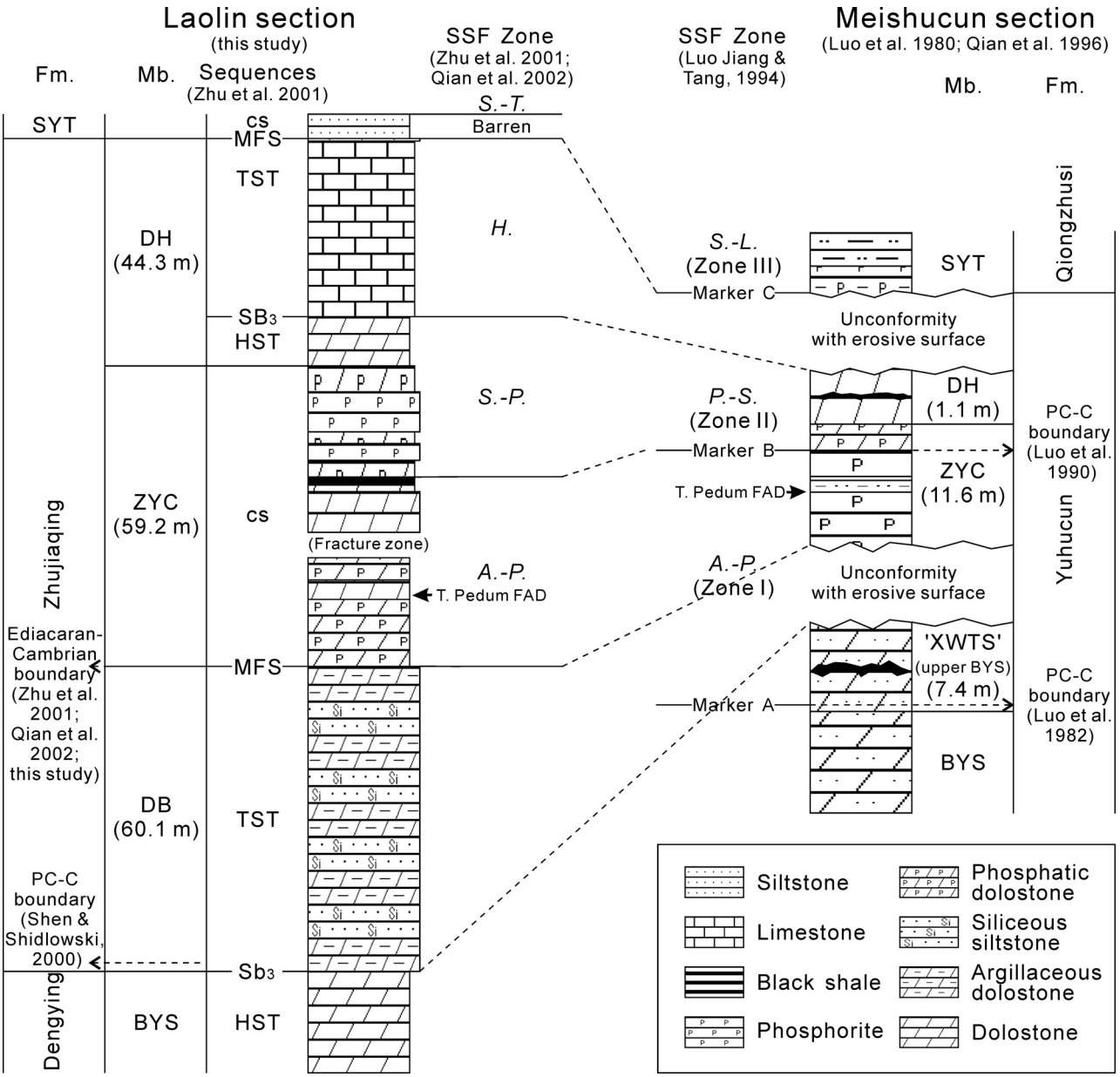

Figure 2. Comparative stratigraphic columns between Laolin section and Meishucun section in Yunnan, SW China. Note the scale of the two sections is not equal. BYS – Baiyanshao Member; DB – Daibu Member; ZYC – Zhongyicun Member; DH – Dahai Member; SYT – Shiyantou Formation. HST – highstand systems tract; SB_3 – third-order sequence boundary; TST – transgressive systems tract; MFS – maximum flooding surface; cs – condensed section. Small shelly fossil (SSF) zones of Laolin section: *A.-P.* – *Anabarites trisulcatus–Protohertzina anabarica* Assemblage; *S.-P.* – *Siphogonuchites triangularis–Paragloborilus subglobosus* Assemblage; *H.* – *Heraultipegma yunnanensis* Assemblage; *S.-T.* – *Sinosachites flabelliformis–Tannuolina Zhangwentangi* Assemblage. SSF zones of Meishucun section: *A.-P.* (Zone I) – *Anabarites–Protohertzina* Assemblage, *P.-S.* (Zone II) – *Paragloborilus–Siphogonuchites* Assemblage, *S.-L.* (Zone III) – *Sinosachites–Lapworthella* Assemblage.

uneven karstic surface of the 'Xiaowaitoushan Member' reached up to 4 m, and phosphorite deposition of the Zhongyicun Member filled the karstic caves and some relatively more dissolved dolomitic beds wihtin the 'Xiaowaitoushan Member' (Qian *et al.* 1996).

The Zhongyicun Member (11.6 m) of the Meishucun section comprises thin (< 0.1 m) to intermediate beds of phosphorite having oölitic microstructure and phosphatic dolostone with some intercalated chert beds in the uppermost part. According to Luo *et al.* (1980, 1990) and Luo, Jiang & Tang (1994), the lower Zhongyicun Member preserves rich small shelly fossils of the *Anabarites–Protohertzina* Assemblage (Zone I) and the upper Zhongyicun Member plus Dahai Member is rich in small shelly fossils of the *Paragloborilus–Siphogonuchites* Assemblage (Zone II). The Dahai Member (1.1 m) comprises grey thin–intermediate dolostone with some chert plates (Luo *et al.* 1982) and is considered later to be disconformably overlain by the Shiyantou Member (He, 1989; Qian *et al.* 1996; Zhu *et al.* 2001; Fig. 2, see details below). The Shiyantou Member (54 m) begins with a more siliciclastic sedimentary unit and comprises black thin beds of phosphatic–argillaceous

https://doi.org/10.1017/S0016756809006268 Published online by Cambridge University Press

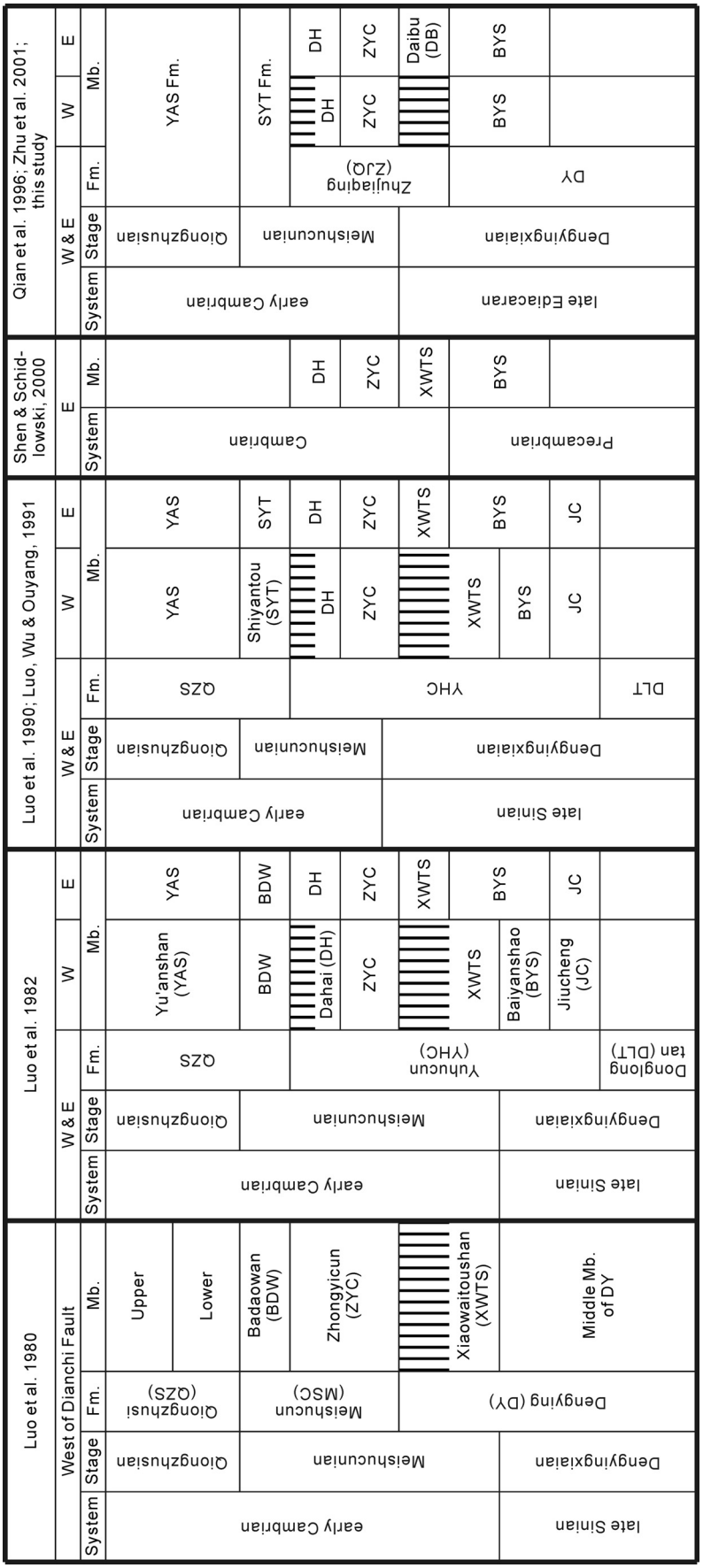

Figure 3. Stratigraphic classification for strata across the Ediacaran–Cambrian boundary in regions east and west of the Dianchi Fault in eastern Yunnan. Formation and member names are abbreviated after their earliest appearance in this table. Vertical hatching represents depositional break. E – region east to the Dianchi Fault; W – region west to the Dianchi Fault. In the left three panels depositional breaks are added according to Qian *et al.* 1996 and Zhu *et al.* 2001.

https://doi.org/10.1017/S0016756809006268 Published online by Cambridge University Press

siltstone in the lower part and grey thin–intermediate beds of argillaceous siltstone and dolomitic siltstone with minor intercalated beds of phosphatic silt-bearing dolostone in the upper part. This member contains small shelly fossils of the *Sinosachites–Lapworthella* Assemblage (Zone III) which extends into the overlying basal Yu'anshan Member.

The Ediacaran–Cambrian boundary was initially placed at Marker A at the base of the 'Xiaowaitoushan Member' in which the FAD of small shelly fossils had been claimed (Luo *et al.* 1980, 1982) but was subsequently placed at Marker B (that is, at the boundary between the *Anabarites–Protohertzina* zone and the *Paragloborilus–Siphogonuchites* zone) in the upper Zhongyicun Member (Luo *et al.* 1990). As for the C-isotope profile in the Meishucun section, no significant shift is indicated across Marker A at the basal 'Xiaowaitoushan Member', while a negatitive C-isotopic excursion was identified in the middle Zhongyicun Member (Brasier *et al.* 1990; Fig. 6, see details below in Section 4.c).

The Laolin section is located in Laolin Village, Dahai Town, Huize County, about 200 km northeast of the Meishucun section (Fig. 1a). The lithology and fossils of the Laolin section were studied by Luo, Wu & Ouyang (1991), and those of the Zhujiaqing section located ~ 20 km north of the Laolin section were studied by Qian *et al.* (1996, 2002) and Zhu *et al.* (2001). According to Luo, Wu & Ouyang (1991), the Laolin section consists of the Jiucheng, Baiyanshao, 'Xiaowaitoushan', Zhongyicun, Dahai, Shiyantou and Yu'anshan members, in upwards order. The Jiucheng Member comprises dark green dolomitic–argillaceous shale and black quartzose siltstone with minor intercalated beds of grey cryptocrystalline dolostone (Luo, Wu & Ouyang, 1991). The Baiyanshao Member comprises grey to dark grey thickly bedded to massive dolostone (Luo, Wu & Ouyang, 1991; this study). The lower part of the 'Xiaowaitoushan Member' comprises sandy–argillaceous dolostone (online Appendix Fig. A2a, http://www.journals.cambridge.org/geo) (Luo, Wu & Ouyang, 1991), which is similar to the Baiyanshao Member in lithology, and according to Qian *et al.* (1996) and Zhu *et al.* (2001) should belong to the Baiyanshao Member. The upper part of the 'Xiaowaitoushan Member' comprises interbedded thin–intermediate, dark, dolomitic cherts and yellowish siliceous dolostone (Luo, Wu & Ouyang, 1991; this study, online Appendix Figs A1d, A2b), and was renamed the Daibu Member by He, Shen & Yin (1988), He (1989) and Qian *et al.* (1996). Zhu *et al.* (2001) suggest that the name 'Xiaowaitoushan Member' be discarded, as it is not equivalent to the Daibu Member. The Daibu Member is a widespread lithostratigraphic unit representing a transgressive systems tract (TST) in NE Yunnan but is absent in the Meishucun area (Qian *et al.* 1996; Zhu *et al.* 2001).

The lower part of the Zhongyicun Member at the Laolin section comprises grey thick beds of laminated phosphorite (online Appendix Fig. A2c) containing Meishucun Zone I-type small shelly fossils of *Anabarites trisulcatus, Protohertzina anabarica, Conotheca subcurvata* and *Olivooides blandes* (Luo, Wu & Ouyang, 1991), which is essentially the same as the *Anabarites trisulcatus–Protohertzina anabarica* Assemblage in the Zhujiaqing section (Qian *et al.* 2002; Zhu *et al.* 2001). The middle part comprises interbedded black thinly bedded argillaceous dolostone and dolomitic oölitic phosphorite (online Appendix Figs A1c, A2d). The upper part comprises light grey to black, thinly to thickly bedded dolomitic phosphorite (online Appendix Fig. A2f) with minor intercalated very thin layers of shale (online Appendix Fig. A2e). The upper Zhongyicun part is rich in Meishucun Zone II-type small shelly fossils of the *Paragloborilus–Siphogonuchites* Assemblage (Luo, Wu & Ouyang 1991), which was revised as the *Siphogonuchites triangularis–Paragloborilus subglobosus* Assemblage by Zhu *et al.* (2001) and Qian *et al.* (2002), based on investigations of the Zhujiaqing section. Marker B is placed at the FAD of *Siphogonuchites–Paragloborilus* Zone small shelly fossils within layer 16 in the upper part of the Zhongyicun Member (Luo, Wu & Ouyang, 1991). The Zhongyicun Member contacts the Daibu Member below and the Dahai Member above, both with transitional boundaries. While chert content gradually decreases and phosphate content increases from the Daibu Member to the Zhongyicun Member, phosphate content decreases and dolomite content increases from the Zhongyicun Member to the Dahai Member. The phosphorite in the Zhongyicun Member represents a condensed section overlying a maximum flooding surface (Zhu *et al.* 2001). At the Laolin section, a fault fracture zone was observed in the upper Zhongyicun Member by this study (Figs 1b, 2).

Luo, Wu & Ouyang (1991) described the lithology of the Dahai Member as dolostone in its lower part and dolomitic limestone in its upper part, and observed Meishucun Zone II-type small shelly fossils of *Paragloborilus, Siphogonuchites, Turcutheca, Hyolithellus, Palaeosulcachites, Sachites, Archaeoides, Cancelloria, Eiffella, Onychia* in this member. According to Qian *et al.* (1996) and Zhu *et al.* (2001) and confirmed by this study, the lower part of the Dahai Member in this region comprises whitish, thickly bedded dolostone and calcitic dolostone (online Appendix Fig. A2g), and the upper part comprises grey thickly bedded to massive argillaceous dolomitic limestone (online Appendix Figs A1b, A2h, i). This member is divided by a third-order sequence boundary into two parts, and the lower dolostone represents highstand systems tract (Zhu *et al.* 2001). In the upper part of the Dahai Member, a new small shelly fossil assemblage zone, the *Heraultipegma yunnanensis* Assemblage Zone, was established by Qian *et al.* (1996, 2002) and Zhu *et al.* (2001), based on investigation of the Zhujiaqing section.

The Shiyantou Member comprises grey to dark grey, thickly to thinly bedded quartz siltstone (online

https://doi.org/10.1017/S0016756809006268 Published online by Cambridge University Press

Appendix Figs A1a, A2j) with excellent stratification (Luo, Wu & Ouyang, 1991), which represents a condensed section, and contains a *Sinosachites–Tannuolina* fossil assemblage (Zhu *et al.* 2001; Qian *et al.* 2002) that extends to the basal Yu'anshan Member. Trilobites first occur at the base of the Yu'anshan Member (Qian *et al.* 2002), which overlies the Shiyantou Member.

As shown in Figure 3, originally, the Zhongyicun, Dahai and Badaowan members were placed into the Meishucun Formation (Luo *et al.* 1980). However, the Badaowan Member (that is, Shiyantou Member) and Yu'anshan Member were subsequently placed into the Qiongzhusi Formation (Luo *et al.* 1982), while the lower Meishucun Formation (Zhongyicun Member and Dahai Member only) and the upper Dengying Formation (including the Jiucheng, Baiyanshao and Xiaowaitoushan members) were combined to form the Yuhucun Formation (e.g. Luo *et al.* 1982; Luo, Wu & Ouyang, 1991; Luo, Jiang & Tang, 1994).

Based on their review of previous investigations and their own studies on sections in eastern Yunnan, Zhu *et al.* (2001) suggested that the name of the Meishucun Formation be changed to Zhujiaqing Formation, which is redefined to include the Daibu, Zhongyicun and Dahai members. This renaming was conceived to avoid possible confusion with the biostratigraphic Meishucunian Stage. Zhu *et al.* (2001) further suggested that the Qiongzhusi Formation be divided into the Shiyantou Formation and the Yu'anshan Formation, in order to avoid confusion with the biostratigraphic Qiongzhusian (Chiungchussuan) Stage. The names 'Xiaowaitoushan Member' and Yuhucun Formation were discarded; the reasons for the former were mentioned above, and the latter was rejected because it spanned too many strata, from the Precambrian to Cambrian.

As well as these nomenclatural changes, Zhu *et al.* (2001) and Qian *et al.* (2002) also revised the fossil assemblages (see above) and fossil zone positions. The base of Zone I has been moved from the 'Xiaowaitoushan Member' to the basal Zhongyicun Member; Zone II, which includes the upper Zhongyicun Member and the Dahai Member, is now divided into two zones: the *Siphogonuchites triangularis–Paragloborilus subglobosus* Zone in the upper Zhongyicun Member and lower Dahai Member and a newly established *Heraultipegma yunnanensis* Zone in the upper Dahai Member. We consider this revised stratigraphic framework and nomenclature (Zhu *et al.* 2001) to be more reasonable than that previously proposed and thus it is adopted in this paper. However, the name 'Xiaowaitoushan Member' with quotation marks is still used in the following text of this paper when reference to the published literature is made, in which case it refers to the Daibu Member in NE Yunnan (including the Laolin and Xiaotan section) and represents only the upper part of the Baiyanshao Member in Kunming area (including the Meishucun section).

The detailed differences between the Meishucun section and the sections in NE Yunnan were first revealed by Qian *et al.* (1996) and Zhu *et al.* (2001). In the region west of the Dianchi Fault (Fig. 1), including the Kunming area, depositional breaks exist between the top Baiyanshao Member and the Zhongyicun Member, and between the Dahai Member and the Shiyantou Formation, while in the region east of the Dianchi Fault, which comprises NE Yunnan Province, sedimentary strata from the Ediacaran–Cambrian boundary interval are generally thicker and more continuous (Qian *et al.* 1996). As a consequence, the Daibu Member and the upper Dahai limestone observed in NE Yunnan (He, Shen & Yin, 1988; He, 1989; Qian *et al.* 1996), and also at the Laolin section (this study) are absent at the Meishucun section (Qian *et al.* 1996). Likewise, the *Heraultipegma yunnanensis* small shelly fossil Assemblage Zone (Fig. 2) found in the upper Dahai Member in eastern Yunnan (Qian *et al.* 2002) is absent in the Kunming region (Luo *et al.* 1990). Based on extensive field work, Qian *et al.* (1996) concluded that the best sections with more continuous deposition and fossils are located near Dahai Town and Yulu Town in Huize County (Fig. 1). While small shelly fossils have not been reported from the Daibu Member at the Laolin and Zhujiaqing sections (Luo, Wu & Ouyang, 1991; Qian *et al.* 2002; this study), small shelly fossils were claimed to be found within the 'Xiaowaitoushan Member' at the Meishucun section (Luo *et al.* 1980). This, however, has not been verified and may represent karstic infillings of the Zhongyicun Member deposition (Qian *et al.* 1996).

2.b. The root of debates about the Laolin section

According to Luo, Wu & Ouyang (1991), no small shelly fossils were found within the 'Xiaowaitoushan Member' at Laolin, yet they placed Marker A at the base of the 'Xiaowaitoushan Member' in their figure 1 without further explanation. They did so possibly by lithological correlation with the Meishucun section where Marker A had been placed at the base of the 'Xiaowaitoushan Member' within which small shelly fossils had been claimed (Luo *et al.* 1980). However, as pointed out above, the small shelly fossils in the 'Xiaowaitoushan Member' at the Meishucun section were not subsequently verified (Qian *et al.* 1996). This discrepancy led subsequently to the debate between Shen & Schidlowski (2000, 2001) and Zhu, Li & Zhang (2001) over the stratigraphic framework and corresponding $\delta^{13}C$ curve at the Laolin section. Shen & Schidlowski (2000) cited the placement of Marker A in figure 1 of Luo, Wu & Ouyang (1991). Zhu, Li & Zhang (2001) argued that Marker A should be placed within the Zhongyicun Member because it was in this member that small shelly fossils first appeared (see text of Luo, Wu & Ouyang, 1991). We thoroughly examined the whole paper of Luo, Wu & Ouyang (1991) and found neither mention of small shelly fossils in the 'Xiaowaitoushan Member' nor any discussion

https://doi.org/10.1017/S0016756809006268 Published online by Cambridge University Press

about the placement of Marker A in their figure 1 as representing the FAD of small shelly fossils at Laolin. During our field study and thin-section observations, we did not find any small shelly fossil within the interval from the upper Baiyanshao Member to the Daibu Member. For the Laolin section, small shelly fossils of *Anabarites, Protohertzina, Conotheca* and *Olivooides* characteristic for the *Anabarites–Protohertzina* Zone have been found in the lower part of the Zhongyicun Member (Luo, Wu & Ouyang, 1991), but no small shelly fossils have been found in the 'Xiaowaitoushan Member' (Luo, Wu & Ouyang, 1991) or in the Daibu Member (this study). Therefore, we agree with the view of Zhu, Li & Zhang (2001) that Marker A, which is palaeontologically defined as the base of small shelly fossil Zone I, should be placed at the base of the Zhongyicun Member (Fig. 2). Such placement is consistent with the study of the Meishucun section (Qian *et al.* 1996) at which the real FAD of small shelly fossils is not in the 'Xiaowaitoushan Member' but in the basal Zhongyicun Member.

In addition, as pointed out by Zhu *et al.* (2001), Shen & Schidlowski (2000) did not mention the limestone unit which is the upper part of the Dahai Member in the Laolin section, and may have not sampled it.

3. Analytical methods

Samples were collected from the upper Baiyanshao Member through to the Daibu, Zhongyicun and Dahai members at Laolin section. Sample lithologies included dolostone of the Baiyanshao Member, dolomitic chert of the Daibu Member, phosphatic dolostone, dolomitic phosphorite and cherty dolostone of the Zhongyicun Member, dolostone, limestone of the Dahai Member, and siltstone of the Shiyantou Formation (Table 1). Thin-sections of the rock samples were scrutinized under a polarizing microscope in order to avoid visible alterations such as micro-vein of calcite and recrystallized calcite in samples destined for element and isotope analyses. Samples of thin-section counterparts without visible alteration were powdered and reacted with orthophosphoric acid at 70 °C for 1 hour to extract CO_2 following the principles first determined by McCrea (1950) and Craig (1953). C- and O-isotope compositions of the liberated CO_2 were measured using a Finnigan MAT-252 mass spectrometer. Chinese GBW00405 carbonate standards (TTB-1 and TTB-2) were placed after every ten samples for checking for memory effects and isotopic calibration. The phosphoric acid-dolomite fractionation factor of 1.01066 (Rosenbaum & Sheppard, 1986) was used for $\delta^{18}O$ calculation. Isotopic data were presented relative to the V-PDB standard. C- and O-isotope compositions of a second sample batch were determined using an online analysis system, Finnigan Gasbench II + Delta Plus XP. The deviations of C- and O-isotope results of repeated measurements on standards are both within 0.15 ‰. The results of duplicate samples agree well within error (Table 1).

A portion of the individual samples was leached by 1M acetic acid at 50 °C for at least 12 hours with several sessions of ultrasonic stirring. The leachate was converted to nitric acid solution by evaporation and redissolution and Rh was added for instrument calibration. Trace element concentrations were determined using a Finnigan Element II ICP-MS. The precisions are generally better than 5 % for the analysed elements based on long-term uncertainty of the lab measurement on standard carbonate.

XRD measurements were carried out using a Rigaku D/max IIIa diffractometer equipped with a Cu-target tube and a curved graphite monochromator, and operating at 37.5 kV, 20 mA. The slit system was 1° (DS/SS), 0.3 mm RS. Samples were step-scanned with a step size of 0.02° (2q) from 18° to 100° and speed of 2s/step. The quantitative mineral phase analysis was achieved by means of Whole Pattern Fitting with a General Structural Analysis System (Larson & Von Dreele, 2004).

All the above analyses were done at the State Key Laboratory for Mineral Deposits Research, Nanjing University.

4. Results and discussion

4.a. Evaluation of diagenesis

Table 1, Figure 4 and Figure 5 show the results for $\delta^{13}C$, $\delta^{18}O$, Mn/Sr and mineral contents of the Baiyanshao Member to basal Shiyantou Formation at the Laolin section. The Mn/Sr ratios of samples from the Baiyanshao Member (except one sample, LL-1), the Daibu Member (except one sample, LL-24), the lower part of Zhongyicun Member and the upper part of the Dahai Member are all below 10. Samples from the upper Zhongyicun Member and the lower Dahai Member have Mn/Sr ratios greater than 10, which may indicate the influence of diagenesis in these units. If diagenesis influenced Mn/Sr, $\delta^{13}C$ and $\delta^{18}O$ equally but affected different samples to different degrees, then negative correlations between Mn/Sr and $\delta^{18}O$, and between Mn/Sr and $\delta^{13}C$, would be expected. However, cross-plots of Mn/Sr–$\delta^{13}C$ and Mn/Sr–$\delta^{18}O$ do not show any correlations (Fig. 4a, b). For the samples with Mn/Sr < 25, their $\delta^{13}C$ and $\delta^{18}O$ vary within a large range without any correlation with Mn/Sr. For the samples with a high and large range of Mn/Sr (30–180), their $\delta^{13}C$ and $\delta^{18}O$ values are intermediate in the whole range of all samples from the section and only vary within a limited range (Fig. 4a, b). Taken individually, no member of the Laolin section shows any such negative correlation either, which suggests that the Mn/Sr ratio may not be a good tracer of diagenetic alteration in this area.

Diagenesis usually causes $\delta^{13}C$ and $\delta^{18}O$ depletion, so positive correlation between $\delta^{13}C$ and $\delta^{18}O$ has often been interpreted as indicating diagenetic resetting (e.g. Bathurst, 1975). Consequently, the $\delta^{13}C$ values of samples with $\delta^{18}O < -10$ ‰ were often thought of as

https://doi.org/10.1017/S0016756809006268 Published online by Cambridge University Press

Table 1. Analytical results for carbonate carbon and oxygen isotope compositions and leachable Mn and Sr concentrations of samples from the Laolin section

Sample no.		Lithology	Height (m)	$\delta^{13}C$ (PDB, ‰)	$\delta^{18}O$ (PDB, ‰)	Mn (ppm)	Sr (ppm)	Mn/Sr	Apatite (%)	Quartz (%)	Calcite (%)	Dolomite (%)
Shiyantou (SYT) Formation												
DH-1	*	calcareous siltstone	188.9	−4.25	−13.33	4278	324.2	13.2	0	26.2	7.4	0
duplicate	*			−4.10	−13.37							
DH-2		siltstone	185.6	b.d.l.	b.d.l.	280.6	271.0	1.03				
DH-3		siltstone	185.0	b.d.l.	b.d.l.	161.2	77.2	2.09				
Dahai (DH) Member, Zhujiaqing Formation												
DH-4		phosphorite	184.0	−5.95	−15.12	810.7	460.9	1.76	44.6	1.2	0	0
DH-5	*	dolomitic limestone	183.2	−1.32	−13.61	582.0	410.5	1.42				
DH-6	*	dolomitic limestone	182.2	1.22	−11.83	751.9	780.8	0.96				
DH-8		dolomitic limestone	178.4	1.32	−13.36	428.6	593.2	0.72	0	5.9	72.9	5.7
DH-9	*	dolomitic limestone	177.3	1.71	−11.29	742.7	681.0	1.09				
DH-10		dolomitic limestone	176.0	3.35	−13.21	308.1	827.3	0.37				
DH-11	*†	dolomitic limestone	174.6	3.47	−13.10	421.2	944.4	0.45	0	9.8	80.4	9.8
DH-12		dolomitic limestone	173.4	3.36	−13.15	334.1	1127	0.30				
DH-13		dolomitic limestone	171.8	2.95	−12.97	508.1	745.3	0.68				
DH-14	†	dolomitic limestone	170.2	1.97	−11.75	1157	269.5	4.29	0	6.0	56.0	36.0
DH-15	*†	calcitic dolostone	168.8	3.45	−13.22	1149	321.1	3.58	3.2	12.6	38.7	44.5
DH-17	*	calcitic dolostone	164.5	2.37	−11.54	2464	107.8	22.9				
DH-18		calcitic dolostone	163.1	1.77	−10.05	2436	124.2	19.6				
DH-19	*	calcitic dolostone	160.8	1.54	−11.19	2355	130.4	18.1	0	17.3	3.0	79.7
DH-20		calcitic dolostone	159.0	0.55	−9.92	2796	157.1	17.8				
DH-21	*	calcitic dolostone	156.0	−0.02	−10.80	1796	133.8	13.4				
DH-23		calcitic dolostone	153.4	−1.30	−8.60	1990	91.43	21.8	5.7	20.1	6.7	54.9
DH-24	*	dolostone	152.8	−0.92	−9.77	2375	103.4	23.0				
DH-25		dolostone	152.4	−0.15	−10.51	2212	108.7	20.3	4.9	32.7	0	45.6
DH-27	*	dolostone	148.1	−0.65	−10.09	530.5	34.6	15.3				
DH-28		dolostone	146.7	−0.50	−8.93	928.8	47.3	19.6				
DH-29	*	dolostone	145.1	0.10	−10.17	592.6	35.9	16.5	0	5.9	0 .7	90.2
DH-30		dolostone	143.6	−0.28	−8.08	713.1	37.3	19.1				
DH-31		dolostone	142.0	−0.65	−7.61	9336	118.5	78.8	0	9.9	0	89.9
Zhongyicun (ZYC) Member, Zhujiaqing Formation												
DH-32		phosphatic dolostone	139.0	−3.16	−8.21	7042	85.3	82.6	8.1	28.0	0	59.1
DH-33		phosphatic dolostone	137.0	−3.79	−8.23	7339	78.8	93.1	16.6	36.1	0	40.3
DH-34	*†	phosphatic dolostone	136.5	−3.45	−11.28	8003	80.7	99.2	32.6	9.9	0	57.5
DH-35		dolomitic phosphorite	135.5	−5.10	−10.63	8147	472.9	17.2	59.6	5.9	0	6.9
DH-36	*	dolomitic phosphorite	132.9	−4.79	−13.02	9195	472.3	19.5	78.4	15.0	0	6.6
duplicate	*			−4.96	−12.59							
DH-37		dolomitic phosphorite	129.5	−4.79	−10.34	14500	210.9	68.8	61.3	14.8	0	24.3
DH-38	*	phosphatic dolostone	127.5	−4.17	−10.93	14681	138.6	105.9	10.2	33.4	0	36.2
DH-39		phosphatic dolostone	125.2	−4.05	−9.68	13500	74.4	181.5	3.3	29.1	0	63.0
DH-40	*†	phosphatic dolostone	124.4	−3.29	−11.45	11612	154.0	75.4	32.3	26.6	0	41.1
DH-41		phosphatic dolostone	123.6	−3.60	−9.22	14000	110.9	126.2	26.0	24.2	0	48.6
DH-42	*	dolomitic phosphorite	122.7	−3.89	−10.09	9342	209.8	44.5	6.6	36.9	0	14.1
DH-43		phosphatic dolostone	118.6	−3.37	−8.36	10900	101.9	107.0	8.6	31.0	0	44.1
DH-44	*	phosphatic chert	116.2	−8.43	−15.14	830.6	551.9	1.51	14.4	33.3	0	0

Table 1. (*cont.*)

Sample no.		Lithology	Height (m)	$\delta^{13}C$ (PDB, ‰)	$\delta^{18}O$ (PDB, ‰)	Mn (ppm)	Sr (ppm)	Mn/Sr	Apatite (%)	Quartz (%)	Calcite (%)	Dolomite (%)
duplicate	*			−8.20	−14.64							
DH-45		cherty phosphorite	115.5	−7.07	−13.96	5868	710.9	8.25	47.0	26.1	0	1.9
DH-46	†	dolostone	113.5	−3.34	−9.26	9817	121.7	80.7	8.7	7.4	0	83.9
DH-48		cherty dolostone	109.3	−2.56	−9.81	6750	170.3	39.6	7.3	21.4	0.9	51.3
DH-49		cherty dolostone	107.8	−0.38	−8.96	3432	149.5	22.9	7.0	16.9	5.1	55.9
DH-50	†	cherty dolostone	106.5	−0.09	−6.64	2740	171.4	16.0	7.6	17.9	10.8	63.7
LL-34	*†	phosphatic dolostone	98.6	−2.15	−13.96	2838	62.2	45.6	5.8	2.2	8.2	83.8
LL-33		dolostone	95.5	−0.31	−10.71	794.6	347.7	2.29				
LL-32	†	dolomitic limestone	94.7	−0.49	−11.26	748.4	523.8	1.43	7.9	10.0	71.3	10.8
LL-31	†	phosphatic limestone	91.8	−1.34	−9.80	1226	297.0	4.13	21.9	23.8	32.7	21.6
LL-30		phosphatic limestone	91.4	−0.44	−10.76	603.1	760.2	0.79	31.3	11.1	42.0	2.3
duplicate	*			−0.40	−11.46							
LL-29		phosphatic dolostone	89.5	−1.64	−9.13	2169	266.3	8.14	25.6	23.7	1.8	33.2
LL-28	†	phosphatic dolostone	87.2	−2.69	−10.69	598.5	400.2	1.50	12.9	4.9	77.4	4.8
LL-27	*†	phosphatic dolostone	82.6	−3.09	−11.78	761.4	428.8	1.78	7.9	7.1	80.0	5.0
LL-26	†	phosphatic dolostone	81.4	−1.84	−10.79	1130	661.3	1.71	8.0	9.6	78.2	4.2
LL-25	†	dolomitic phosphorite	80.3	−2.95	−10.43	1276	312.9	4.08	41.6	8.0	35.6	14.8
Daibu (DB) Member, Zhujiaqing Formation												
LL-24	*	argillaceous dolostone	79.8	−0.97	−10.22	4579	79.5	57.6	12.1	17.5	0.9	63.3
LL-22		dolomitic chert	58.8	−5.79	−11.91	1475	246.4	5.99	0	68.7	9.3	4.6
LL-21		dolomitic chert	57.8	−4.21	−10.43	2139	572.9	3.73	2.4	80.6	0	8.2
LL-20		dolomitic chert	54.9	−6.31	−8.74	877.6	276.7	3.17	0	46.4	0.8	8.5
LL-18	*	dolomitic chert	49.5	−6.39	−10.45	1455	459.3	3.17	0	72.7	2.0	8.5
LL-17		dolomitic chert	47.4	−6.65	−10.12	3701	1269	2.92	0	67.1	7.3	9.5
LL-16		dolomitic chert	46.1	−11.00	−7.22	365.3	499.6	0.73	0	47.2	0.9	8.7
duplicate	*			−10.92	−8.33							
LL-15	*	dolomitic chert	42.6	−7.00	−11.04	924.2	557.9	1.66	0	75.3	8.6	10.6
LL-14		dolomitic limestone	41.6	−6.53	−9.63	755.2	872.8	0.87	0	21.1	50.9	28.2
LL-13		dolomitic chert	40.0	−7.24	−9.45	1044	679.2	1.54	0	50.7	14.7	21.0
Baiyanshao (BYS) Member, Dengying Formation												
LL-11		dolostone	19.8	−2.31	−7.19	114.7	38.3	2.99				
LL-10	†	dolostone	17.9	−2.46	−7.46	97.6	39.7	2.46	0	2.5	0	97.5
LL-9		dolostone	16.2	−1.73	−7.49	135.0	126.0	1.07				
LL-8		dolostone	14.7	−1.08	−7.44	130.5	137.5	0.95				
LL-7	*	dolostone	13.3	−1.45	−9.41	133.3	208.6	0.64				
LL-6	†	dolostone	11.6	−0.87	−7.79	188.6	206.4	0.91	0	3.6	1.9	94.5
LL-5	*	dolostone	9.1	1.05	−12.16	227.2	92.2	2.46				
LL-4	*	dolostone	6.5	1.00	−11.43	568.6	95.5	5.95				
LL-3	†	dolostone	4.8	1.42	−12.85	325.2	112.7	2.89	0	6.2	7.3	86.5
LL-1	*	dolostone	1.9	0.51	−11.99	1314	63.5	20.7	0	7.5	2.2	65.1

* $\delta^{13}C$ and $\delta^{18}O$ were analysed with an online Finnigan Gas-Bench + DeltaPlus XP system. $\delta^{13}C$ and $\delta^{18}O$ of the other samples were analysed with a Finngan MAT-252 after offline extraction of CO_2.
b.d.l. – below detectable limit.
† The sums of mineral contents calculated from XRD results are greater than 100%, which occurs when the calculated corundum contents are less than the actual contents of corundum added to the samples, and have been normalized to one hundred percent.

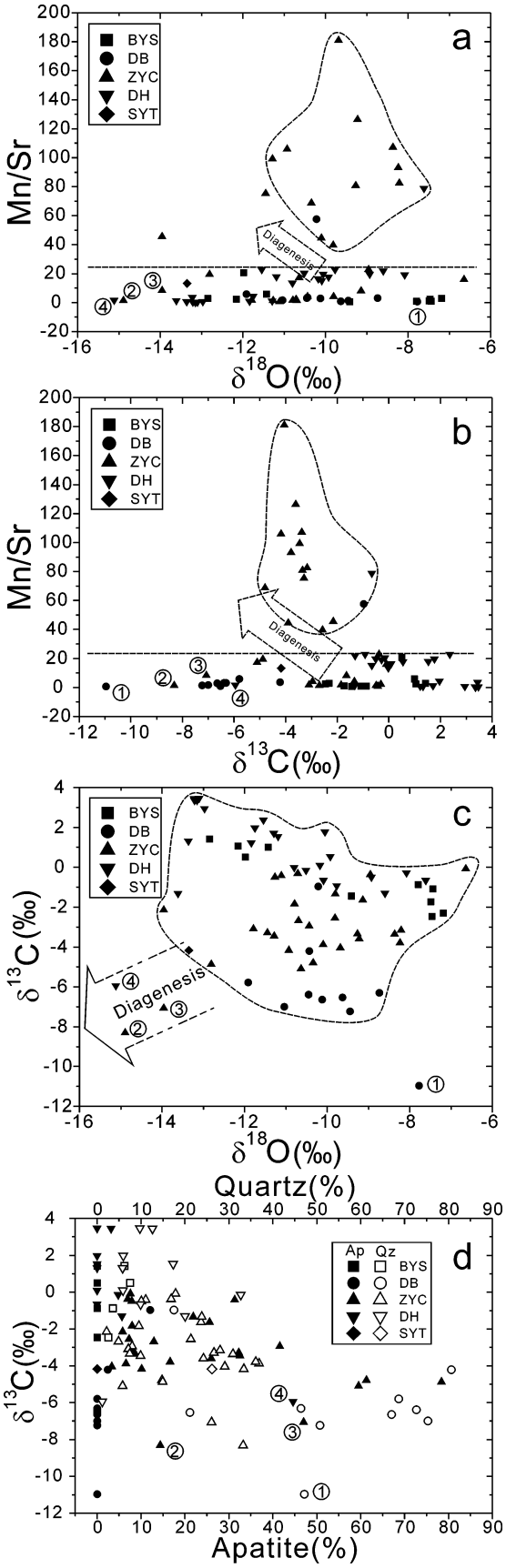

Figure 4. Cross-plots of $\delta^{18}O$–Mn/Sr (a), $\delta^{13}C$–Mn/Sr (b), $\delta^{18}O$–$\delta^{13}C$ (c) and $\delta^{13}C$–phosphate and quartz (d) for Laolin section in northeastern Yunnan, southwestern China. BYS – Baiyanshao Member; DB – Daibu Member; ZYC – Zhongyicun Member; DH – Dahai Member; SYT – Shiyantou Formation. Circled numbers: 1 – Sample LL-16; 2 – DH-44; 3 – DH-45; 4 – DH-4.

having been affected by diagenesis. Nearly half of our $\delta^{18}O$ values are below −10 ‰. However, except for the upper part of the Zhongyicun Member, samples of the Laolin section show no positive correlation between $\delta^{18}O$ and $\delta^{13}C$ (Fig. 4c). The Dahai Member, except for one sample, even shows a clear negative correlation, while the Daibu and Baiyanshao members also show broad negative correlations. Such negative correlations are difficult to reconcile with most diagenetic processes and suggest instead a primary signature. Theoretically, potential reasons for negative correlation could include spatial and/or depth heterogeneity of $\delta^{13}C$ in the water column, although this could not be proven in this study. The strongly negative $\delta^{13}C$ composition (−11.0 ‰) with high $\delta^{18}O$ value (−7.22 ‰) of a sample from the Daibu Member (LL-16, Fig. 4c) is particularly difficult to explain given the mantle input value (Kump, 1991), and would require an additional source of ^{12}C if it were representative of seawater. The oxidation of organic matter might provide the additional ^{12}C, which implies diagenetic alteration. Thus this sample is not included in the evolutionary curve (Fig. 5).

The $\delta^{18}O$ and $\delta^{13}C$ values of two samples from upper part of the Zhongyicun Member (DH-44, DH-45, Fig. 4c) together with one sample of the top Dahai Member (DH-4, Fig. 4c) plot towards the lower left part in the trend arrow in Figure 4c and may have been modified most significantly by diagenesis. In thin-sections of sample DH-44, which is from the sole 1.6 m thick black shale layer in the Zhongyicun Member, carbonate can hardly be seen except in the form of a micro-vein (online Appendix Fig. A2e; also see XRD data in Table 1). Therefore, the measured C-isotope values may have come from diagenetic carbonate. Thin-section observations show that sample DH-45 is unique in our sample set from the Zhongyicun Member for its almost pure granular phosphorite without visible carbonate but with some chert and micro-cavities (online Appendix Fig. A2d; also see XRD data in Table 1); these micro-cavities might have been carbonate once that has been dissolved by meteoric water. Consequently, the $\delta^{13}C$ value of this sample may reflect minor carbonate remnants whose C-isotope composition was affected by meteoric water. For these reasons, in the $\delta^{13}C$ evolutionary diagram (Fig. 5), we abandoned these two upper Zhongyicun Member samples (DH-44, DH-45). Previous study suggests phosphate formation-associated diagenesis could lead to $\delta^{13}C$ depletion (e.g. Brasier *et al.* 1990). The XRD results of the bulk samples from the Laolin section (Table 1), however, show no correlation between $\delta^{13}C$ and apatite contents (Fig. 4d). This suggests that either diagenetic effect on the $\delta^{13}C$ values was not related to the apatite contents, or the $\delta^{13}C$ values of the studied samples were not significantly affected by diagenesis and thus reflected an approximation to the primary record. Other indications mentioned above supported the latter scenario. The $\delta^{13}C$ values of the studied samples were not correlated with the silicic content either. This also suggests that the chert-rich dolostone intervals (mainly

https://doi.org/10.1017/S0016756809006268 Published online by Cambridge University Press

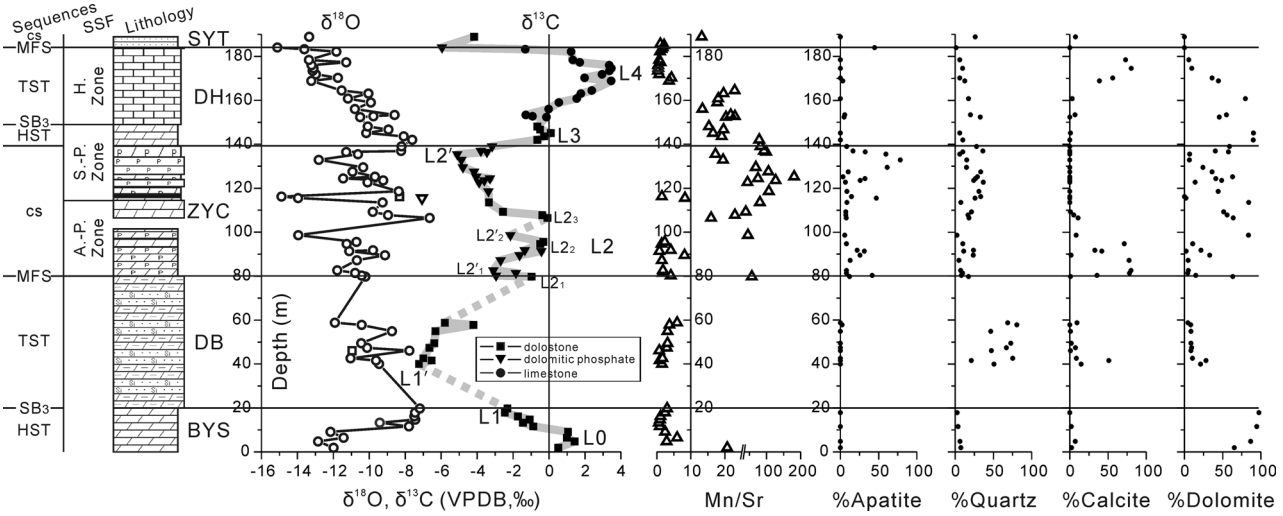

Figure 5. Profiles of $\delta^{13}C$, $\delta^{18}O$, Mn/Sr and XRD data for Laolin section in Yunnan, southwestern China. Small shelly fossils (SSF) zones: A.-P. Zone – *Anabarites trisulcatus–Protohertzina anabarica* Assemblage Zone; S.-P. Zone – *Siphogonuchites triangularis–Paragloborilus subglobosus* Assemblage Zone; H. Zone – *Heraultipegma yunnanensis* Assemblage Zone. HST – highstand systems tract; SB_3 – third-order sequence boundary; TST – transgressive systems tract; MFS – maximum flooding surface; cs – condensed section. BYS – Baiyanshao Member; DB – Daibu Member; ZYC – Zhongyicun Member; DH – Dahai Member; SYT – Shiyantou Formation. In a couple of sectors indicated by dashed lines, samples are not available due to intensive weathering (from $L2_1$ and from L1′ to the underlying points) or fault fragmentation (from $L2'_2$ to $L2_3$). For lithological legends see Figure 2.

the Daibu Member) recorded approximately primary $\delta^{13}C$ values (Fig. 4d).

4.b. New $\delta^{13}C$ trend and comparison with previous work

After abandoning some samples whose $\delta^{13}C$ values may have been significantly affected by diagenesis, the $\delta^{13}C$ curve of the Laolin section (this study, Figs 5, 6; hereafter Curve II) should represent at least an approximation to the primary $\delta^{13}C$ trend for the Ediacaran–Cambrian boundary interval. The $\delta^{13}C$ trend displayed by this curve can now be compared with the $\delta^{13}C$ curve of Shen & Schidlowski (2000) for the Laolin section (hereafter Curve I; Fig. 6). For Curve II, the $\delta^{13}C$ values of the upper Baiyanshao dolostone show a continuous decline in an upward direction from 1.4 ‰ (L0) to −2.5 ‰ (L1), which is similar to the trend from S0 to S1 of Curve I, although the $\delta^{13}C$ value (L1) of the upper Baiyanshao Member in Curve II is less negative than that of Curve I in the upper Baiyanshao Member (S1). A part of the section between the upper Baiyanshao Member and the lower Daibu Member was covered by talus material during our sampling, and so no samples from this part (which might be expected to have more negative $\delta^{13}C$ values) have been collected. The low $\delta^{13}C$ values of Curve II in the lower–middle Daibu Member (−6.5 to −7.2 ‰, L1′), which is similar to the correlative $\delta^{13}C$ values of Curve I (S1′), are possibly a consequence of the continuation of this general decline from the upper Baiyanshao Member. However, Curve II does not record the abrupt rise at the top of the Baiyanshao Member shown in Curve I. From the middle to the top of the Daibu Member, $\delta^{13}C$ values of Curve II show a rise from the nadir of the curve (L1′) to −1.2 ‰ ($L2_1$), which is also similar to the rise from S1′ to S2 in Curve I.

From S2 and L2 upward, the two curves diverge. For Curve II, in the lower and middle parts of the Zhongyicun phosphorite and phosphatic dolostone, $\delta^{13}C$ values vary in a relatively small range (between −3.2 and 0 ‰) which may include some modest cycles from $L2_1$ to $L2_3$. After this, larger changes occur again. The $\delta^{13}C$ values decline evidently from −0.1 ‰ ($L2_3$) in the middle–upper Zhongyicun Member to −5.1 ‰ (L2′) in the upper Zhongyicun Member. Toward the top of the Zhongyicun Member, $\delta^{13}C$ values rise slightly to −3.2 ‰. The succeeding Dahai dolostone and limestone continue this increasing trend, reaching up to about +3.5 ‰ at the top (L4) of the succession in the upper Dahai Member. In the middle of this approximately 9 ‰ rise there is a small negative shift from +0.1 (L3) to −1.3 ‰. After the apex at +3.5 ‰ (L4), the curve begins to decline toward the top of the Dahai Member and appears to plummet to a very low value of −5.7 ‰ (DH-4) at the Dahai–Shiyantou boundary, although diagenetic alteration of this sample cannot be fully ruled out as pointed out above.

In Curve I (Fig. 6), there are two sectors which distinctly differ from Curve II. (1) In Curve I all $\delta^{13}C$ values of the Zhongyicun Member are below −4.4 ‰ (S2), whereas in Curve II only the upper Zhongyicun Member has comparable negative $\delta^{13}C$ values (L2′) and all of the middle and lower Zhongyicun Member has $\delta^{13}C$ values between −3.2 ‰ and −0.1 ‰ (L2). (2) In Curve I all the $\delta^{13}C$ values of the Dahai Member are below 0 ‰ (S3) whereas in Curve II the $\delta^{13}C$ values of the Dahai Member rise up to a peak at +3.5 ‰ (L4) in the upper part of the member.

https://doi.org/10.1017/S0016756809006268 Published online by Cambridge University Press

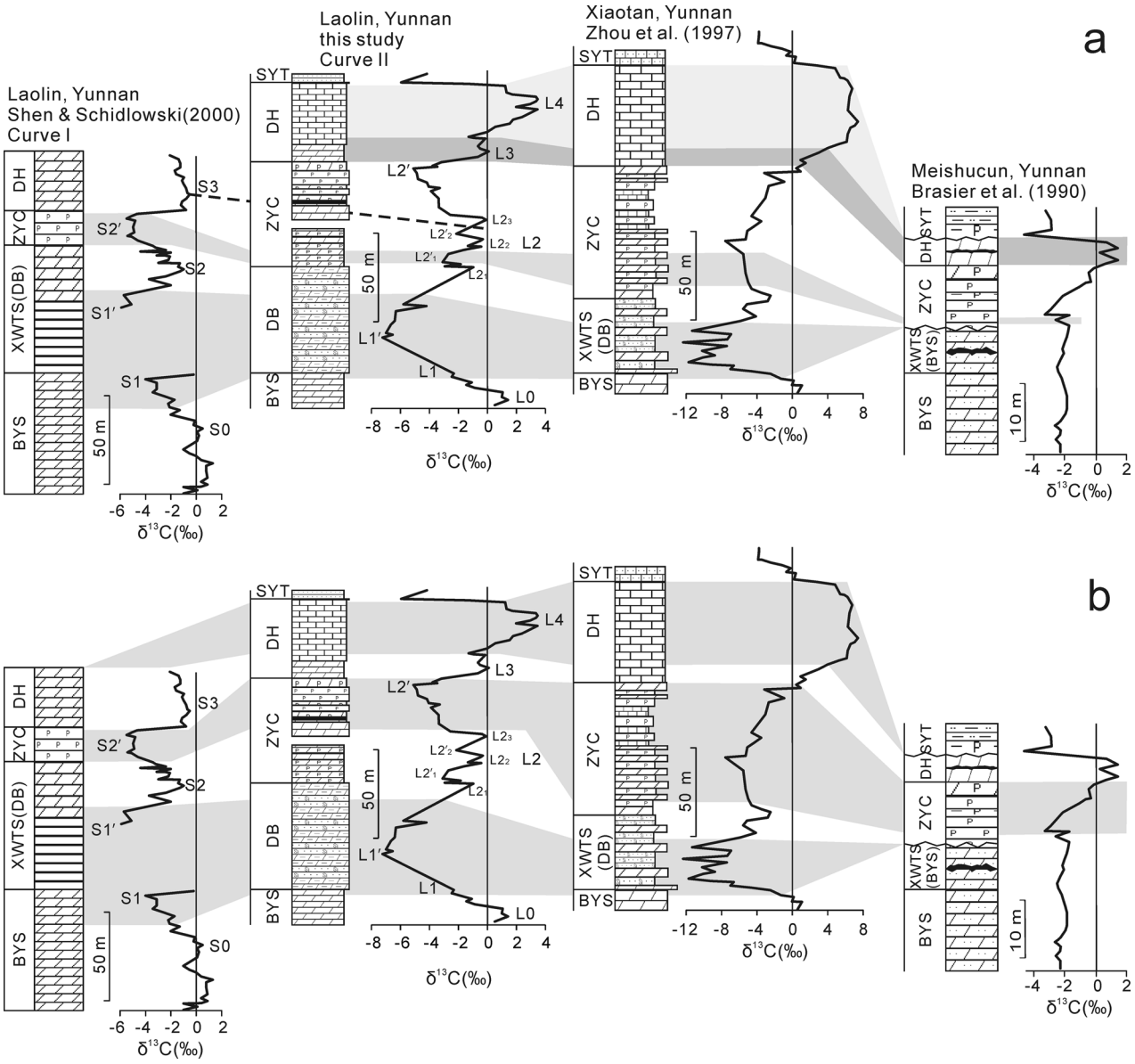

Figure 6. C-isotope stratigraphic correlation scheme between sections on Yangtze Platform. Panels (a) and (b) present two possible ways of correlation; for details see text. Curve I and its labels S1, S2 and S3 are from Shen & Schidlowski (2000). Labels S0, S1′ and S2′ of Curve I are added by this study. Note the scale for the much thinner Meishucun section is not equal to that for the others, and the thicknesses are not proportional to time. BYS – Baiyanshao Member; DB – Daibu Member; ZYC – Zhongyicun Member; DH – Dahai Member; SYT – Shiyantou Formation.

The Zhongyicun Member $\delta^{13}C$ values of Curve I (S2′) seem only to correspond to either the lower Zhongyicun Member (Fig. 6a) or the upper Zhongyicun Member (Fig. 6b) of Curve II. In either case, a part of the Zhongyicun Member seems to be missing or was taken as part of a neighbouring member for Curve I. It cannot be that we have mistaken the Zhongyicun Member in our study because the Zhongyicun Member contains phosphorite or phosphatic dolostone beds throughout its thickness and these are not hard to recognize in the field. Our thin-section work and XRD results verify that almost all samples of the Zhongyicun Member contain phosphate, whereas the underlying Daibu Member and the overlying Dahai Member contain little or no phosphate. Under the assumption that the placement of the boundary between the 'Xiaowaitoushan Member' and the Zhongyicun Member of Curve I is correct, then the Zhongyicun Member of Curve I (S2′) may correspond to the lower Zhongyicun Member ($L2'_1$, Fig. 6a) rather than to the upper Zhongyicun Member (L2′) of Curve II; the alternative possibility of correlating S2′ to L2′ (Fig. 6b) would imply that the lower–middle part of the Zhongyicun Member has been missed during sampling, which would not have happened easily. If S2′ corresponds to $L2'_1$, then S3 may correspond to $L2_2$ and $L2_3$ (Fig. 6a), in which case the real Dahai Member of the section has not been sampled and the 'Dahai Member' of Curve I might in reality be the middle–upper part of the Zhongyicun Member. Such a scenario is not impossible because there is a fault fracture zone in the middle–upper part of the Zhongyicun Member

https://doi.org/10.1017/S0016756809006268 Published online by Cambridge University Press

(Fig. 1b). At this locality, the rocks look like siltstone and could be taken as rock of the Shiyantou Formation.

However, the $\delta^{13}C$ values of the Zhongyicun Member of Curve I (< -4.5 ‰, S2) are more comparable to the upper part of the Zhongyicun Member of Curve II (L2′) (Fig. 6b). Figure 6b shows a more likely correspondence between Curve I and Curve II and a more consistent correlation of the two curves of the Laolin section with other sections in eastern Yunnan. If such correspondence between Curve I and Curve II is correct, then the upper part of the 'Xiaowaitoushan Member' of Curve I should correspond to the lower part of the Zhongyicun Member, while the upper part of the Dahai Member was not sampled for Curve I; this was also suspected by Zhu, Li & Zhang (2001). For these reasons, we consider that the situation shown in Figure 6b is more likely than the situation shown in Figure 6a.

In summary, the new Laolin $\delta^{13}C$ profile shows two pronounced negative excursions (L1′ and L2′) and one pronounced positive $\delta^{13}C$ excursion (L4) with three less pronounced positive $\delta^{13}C$ excursions (L0, L2 and L3). Although in a couple of sectors, samples are not available due to fracturing and weathering, the new C-isotope profile is more detailed than the previously published one (Shen & Schidlowski, 2000) in which the upper Dahai limestone may have been missed and the lower Zhongyicun Member may have been taken as the upper 'Xiaowaitoushan Member'.

4.c. Comparison with C-isotope curves of Xiaotan section and Meishucun section in eastern Yunnan

The C-isotope curve of the Laolin section is very similar to that of the Xiaotan section at Yongshan (Zhou *et al.* 1997) (Fig. 6), ~200 km north of the Laolin section (Fig. 1). The most prominent common features of the two $\delta^{13}C$ profiles are a large negative shift (over 8 ‰) starting at the top of the Baiyanshao Member and ending at the Daibu Member, and a large positive shift (over 8 ‰) starting at the top of the Zhongyicun Member and ending at the Dahai Member, followed by a similarly large negative shift extending to the overlying Shiyantou Formation. The similarity between the $\delta^{13}C$ profiles of the two sections indicates that these units represent chronostratigraphic entities with similar depositional environments, and provides confidence that these curves may provide some correlation potential further afield. The similarities between Curve II of the Laolin section and the C-isotope curve of the Xiaotan section also highlight a probable inaccuracy in Curve I.

Comparison of the C-isotope curves between the sections east of the Dianchi Fault (including the Laolin section from this study and the Xiaotan section) with the Meishucun section west of the fault, shows some similarities and dissimilarities. The similarities include the prominent rise from negative values in the Zhongyicun Member to positive values in the Dahai Member followed by a large fall to the overlying Shiyantou Formation. Luo, Wu & Ouyang (1991) believed the 'Xiaowaitoushan Member' to be equivalent to the Daibu Member, but the most prominent dissimilarity is the lack of a pronounced negative shift in the 'Xiaowaitoushan Member' at the Meishucun section, which supports the above-mentioned view that there is a depositional break between the so-called 'Xiaowaitoushan Member' and the Zhongyicun Member at Meishucun (He, Shen & Yin, 1988; He, 1989; Qian & Bengtson, 1989; Qian *et al.* 1996). According to these papers, at the Meishucun section the 'Xiaowaitoushan Member' is similar to and belongs in the underlying upper Baiyanshao Member which was followed by a depositional hiatus during which time the Daibu Member was deposited in the region east of the Dianchi Fault with a pronounced negative C-isotope shift. A less evident dissimilarity is that the Dahai $\delta^{13}C$ peak at the Meishucun section (< 2 ‰) is not as high as the one at the Laolin section (3.5 ‰), which may also support the above-mentioned claim of another depositional hiatus between the Dahai Member and Shiyantou Formation at the Meishicun section (He, 1989; Qian *et al.* 1996; Zhu *et al.* 2001). It is conceivable that the upper Dahai limestone in the Dahai area was deposited during this interval (Qian *et al.* 1996), although depositional depth differences within the basin could also result in $\delta^{13}C$ variation.

4.d. Global correlations

4.d.1. Ediacaran–Cambrian boundary associated negative $\delta^{13}C$ excursion

As pointed out in Section 1, because the Global Stratotype Section and Point of the Ediacaran–Cambrian boundary at Fortune Head, southeastern Newfoundland, Canada, was established mainly on the basis of trace fossils in siliciclastic strata (Narbonne *et al.* 1987; Landing, 1994), correlation of shallow marine carbonate strata with this stratotype has been difficult. Sections spanning the Ediacaran–Cambrian boundary in south China have not only small shelly fossil zones (e.g. Luo *et al.* 1980; Luo, Wu & Ouyang, 1991; Qian *et al.* 2002) for correlation with worldwide carbonate-dominated regions, but also well-established trace fossil zones (Yin, Li & He, 1993) for correlation with siliciclastic regions, thus providing maximum potential for correlation. Over the past decade it has become increasingly clear that a distinctly large $\delta^{13}C$ negative excursion is closely associated with Ediacaran–Cambrian boundary strata worldwide, such that the negative excursion itself is increasingly regarded as a surrogate for the boundary (Strauss *et al.* 1992, pp. 117–27; Grotzinger *et al.* 1995; Knoll & Carroll, 1999; Kimura & Watanabe, 2001). An attempt at global correlation of the C-isotope curve we obtained for the Laolin section, calibrated with biotratigraphic markers, is made below.

Figure 7 shows our profile together with C-isotope stratigraphic profiles from the Anabar uplift of NW

https://doi.org/10.1017/S0016756809006268 Published online by Cambridge University Press

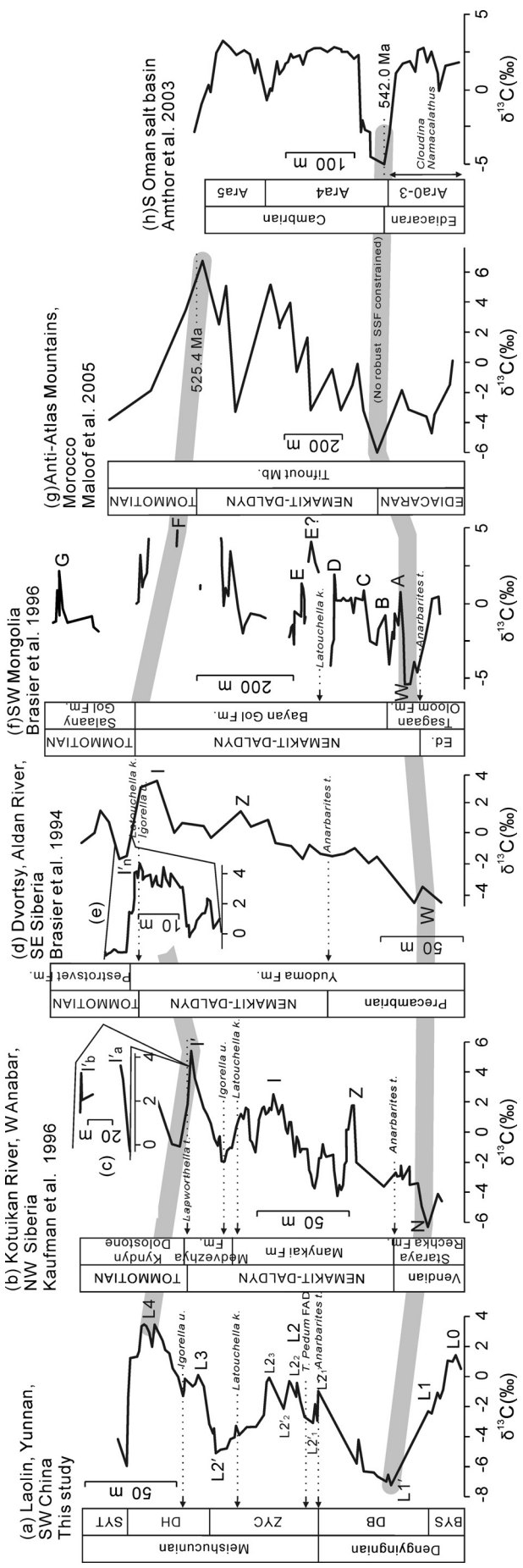

Figure 7. Global C-isotope stratigraphic correlation scheme. Negative $\delta^{13}C$ excursions around the Ediacaran–Cambrian boundary are correlated between L1′ in section (a), N in section (b), W in section (d) and (f), and other two in section (g) and (h). Positive excursions near the base of Tommotian are correlated between L4 in section (a), I′ in section (b), F in section (f) and the one in section (g). Sources of data for each section are indicated. Data of $\delta^{13}C$ curve sector (c) are from Bol'shaya Kuonamka section of E Anabar uplift, NW Siberia (Kouchinsky *et al.* 2001), and $\delta^{13}C$ curve sector (e) from Selinde section, SE Siberia (Kouchinsky *et al.* 2005). Strata from top Manykai to Medvezhya Formation containing I′ deposited at W Anabar uplift, NW Siberia did not deposit in Aldan River section, SE Siberia (Kaufman *et al.* 1996). I'_a, I'_b are correlated with I'_n, and are suggested by the authors to be above I′ in Koutuikan River section, NW Siberia. See text for details. Note only the left three sections have equal scale bars. BYS – Baiyanshao Member; DB – Daibu Member; ZYC – Zhongyicun Member; DH – Dahai Member; SYT – Shiyantou Formation.

https://doi.org/10.1017/S0016756809006268 Published online by Cambridge University Press

Siberia (Kaufman *et al.* 1996; Kouchinsky *et al.* 2001), SE Siberia (Brasier *et al.* 1994; Kouchinsky *et al.* 2005), SW Mongolia (Brasier *et al.* 1996), Morocco (Maloof *et al.* 2005) and southern Oman (Amthor *et al.* 2003).

Cross-correlation between the Mongolian and Siberian profiles is anchored by the negative excursion 'W', Sr isotope stratigraphy, and FAD of skeletal fossils (Brasier *et al.* 1996; Shields, 1999). On the Siberian Platform, the negative $\delta^{13}C$ boundary excursion is situated not far below the FAD of *Anabarites trisulcatus* small shelly fossils at Aldan River (Magaritz, Holser & Kirschvink, 1986; Magaritz *et al.* 1991; Brasier *et al.* 1994), Kotuikan River (Pokrovsky & Missarzhevsky, 1993; Knoll *et al.* 1995*b*; Kaufman *et al.* 1996) and Sukharikha River (Kouchinsky *et al.* 2007). The first negative $\delta^{13}C$ excursion on the Siberia Platform (W in Fig. 7d, −4.5 ‰) was observed by Magaritz, Holser & Kirschvink (1986) in predominantly dolostones of the Yudoma Formation at the Dvortsy section, along the Aldan River, SW Siberia, where the former Precambrian–Cambrian stratotype candidate was proposed (Cowie, 1985). The negative excursion at the Kotuikan River section, Anabar uplift, NW Siberia (N in Fig. 7b, −6.2 ‰) was recorded in massive dololutite in the middle part of the Staraya Rechka Formation, which represented a range of shallow, restricted subtidal to intertidal depositional environments devoid of strong currents (Kaufman *et al.* 1996). The negative excursion (labelled '1n', −8.6 ‰), at the Sukharikha River section on the NW Siberia platform, occurred in the basal Sukharikha Formation consisting of mostly dolostones and subordinate limestones deposited from the proximal carbonate-ramp environment (Kouchinsky *et al.* 2007). A comparable negative excursion (−7 ‰) was observed in the middle part of the Lower Shale Member of the Soltanieh Formation at the Valiabad section, Elburze Mountains, N Iran and was also below the early skeletal fossils, such as *Protohertzina anabarica*, occurring near the top of this member. This negative excursion was recorded in the rhythmically interbedded carbonate-shale layers (< 1 m) in shale successions deposited in an open marine subtidal environment (Brasier *et al.* 1990; Kimura *et al.* 1997). A more negative excursion (−9.3 ‰), situated in the thin beds of lime mudstone sporadically occurring at the base of the Ingta Formation, which consists predominantly of fine siliciclastic rocks on shallow shelf, is directly below the FAD of both body fossils (*P. anabarica*) in the top Ingta Formation and trace fossils (*P. pedum*) in the middle Ingta Formation of the Mackenzie Mountains, NW Canada (Narbonne, Kaufman & Knoll, 1994). The Laolin $\delta^{13}C$ Curve II shows a very similar situation, with a −7.2 ‰ negative excursion (L1′) in the Daibu Member that lies just below the FAD of *Anabarites–Protohertzina* and *T. Pedum* within the basal Zhongyicun Member.

A similar negative $\delta^{13}C$ excursion in the upper Tsagan Oloom Formation, Zavkhan basin, SW Mongolia (feature W, −5.3 ‰), however, lies slightly above the level of the FAD of the *Anabarites trisulcatus* Zone and the earliest assemblage of hexactinellid sponge spicules (Brasier *et al.* 1996). This excursion appears in light- and dark-grey limestone with black siliceous concretions deposited in shelf and peritidal environments. At the Kuorbusuonka River section, Olenek uplift, NE Siberia, a less negative $\delta^{13}C$ excursion (−2.6 ‰) in shallow ramp dolostone of the uppermost Turkut Formation, lies above the lowermost shelly fossil *Cambrotubulus* sp. (Knoll *et al.* 1995*a*; Khomentovsky & Karlova, 1993). A similar negative shift nearby is reported from the upper Turkut Formation at the Olenek River section (−3.5 ‰) (Pelechaty *et al.* 1996; Plechaty, Kaufman & Grotzinger, 1996). These latter two excursions are less negative than the typical negative excursions (< −4 ‰) spanning the Ediacaran–Cambrian boundary around the world.

Although the FADs of small shelly fossils are very likely diachronous (Brasier *et al.* 1996), this almost ubiquitous and large negative $\delta^{13}C$ excursion could be used as a chronostratigraphic anchor for the Ediacaran–Cambrian boundary. Trace fossil data from eastern Yunnan provide further support for this. Yin, Li & He (1993) studied 27 sections distributed over an area of 30 000 km^2 from Huize to Kunming and observed *Phycodes pedum* limited in phosphorites of lower Zhongyicun Member (just above negative $\delta^{13}C$ excursion L1), which could be correlated with *Trichophycus pedum* from the Global Stratotype Section at Fortune Head, SE Newfoundland, Canada.

Supportive data for using this excursion as a global marker also come from other successions in the world without the *Anabarites trisulcatus* Zone. For instance, at the Turukhansk uplift on the northwestern margin of the Siberia Platform, a negative $\delta^{13}C$ excursion (−7.5 ‰) has also been found in subtidal shelf silty dolostone at the lower part of the Platonovskaya Formation, whose trace and body fossils can only broadly constrain the depositional age being around the Ediacaran–Cambrian boundary (Bartley *et al.* 1998). At the Nokhtuisk section on the southern margin of the Siberia Platform, a large and prolonged negative $\delta^{13}C$ excursion interval N1 (−9 ‰) with some superposed high frequency shifts (< 5 ‰), occurring in micritic clasts of carbonate conglomerates spreading over a thick interval (200 m) in the middle and upper Tinnaya Formation deposited on distally steepened ramp in deep water, is just below the red beds of the Nokhtuisk Formation; these do not contain guide fossils but are suggested as being early Cambrian based on regional lithostratigraphic considerations (Pelechaty, 1998). A pronounced negative excursion (−6 ‰) occurring in peritidal dolostones of the lower Tifnout Member in the Ediacaran–Cambrian boundary successions of the Anti-Atlas mountains in Morocco is also inferred to have recorded the same biogeochemical event (Magaritz *et al.* 1991; Maloof *et al.* 2005) (Fig. 7g), although biostratigraphic data only constrain the excursion as post-dating Ediacaran faunas and

https://doi.org/10.1017/S0016756809006268 Published online by Cambridge University Press

pre-dating Atdabanian fossil assemblages of the later early Cambrian (Tucker, 1986; Latham & Riding, 1990).

Recently, precise U–Pb dating on zircons from volcanic ash beds within a stratum coincident with the negative C-isotope excursion (−5 ‰) at the basal A4 carbonate formed during highstands in an unrestricted sea in the southern Oman Salt Basin yielded an age of 542.0 ± 0.3 Ma (Amthor *et al.* 2003; Fig. 7h). This age constraint agrees well with previous constraints for the negative C-isotope excursions around the Ediacaran–Cambrian boundary at Khorbusuonka River, NE Siberia (slightly below the ash bed with a zircon age of 543.9 ± 0.2 Ma: Bowring *et al.* 1993) and S Namibia (between two ash beds with zircon ages of 543.3 ± 1 Ma and 539.4 ± 1 Ma: Grotzinger *et al.* 1995), and provides further support for the global validity of the Ediacaran–Cambrian boundary excursion. The extinction of *Cloudina* and *Namacalathus* occurred close to the Ediacaran–Cambrian boundary in Oman and globally (Amthor *et al.* 2003; Brasier, 1989, pp. 73–88; Seilacher, 1984, pp. 159–68) and appears to have been coincident with the global biogeochemical event marked by the negative C-isotope excursion (Knoll & Carroll, 1999). Therefore, this global biogeochemical event pre-dated the Cambrian bioradiation and may have coincided with mass extinction and faunal turnover at the Ediacaran–Cambrian boundary.

Exceptional cases where no clear negative excursion appears around the supposed Ediacaran–Cambrian boundary have been observed occasionally. Biostratigraphic and chemostratigraphic data for the terminal Neoproterozoic mixed deltaic to shallow marine siliciclastic carbonate successions in Namibia support a latest Vendian age for the top of the Spitskopf Member, but in the overlying strata no negative excursion is observed near the Ediacaran–Cambrian boundary as in other regions, suggesting the youngest Vendian strata were probably removed by erosion or never deposited in the basin (Grotzinger *et al.* 1995). Similarly, in the Meishucun section, a clear negative excursion is also absent below the reported FAD of *Anabarites–Protohertzina* (basal Zhongyicun Member). The negative excursion in the Zhongyicun Member at the Meishucun section should correlate with L2′ in the Zhongyicun Member but not with excursion L1′ in the Daibu Member of the Laolin section. Thus, regardless of whether the *Anabarites–Protohertzina* fossils from the 'Xiaowaitoushan Member' are of primary (Luo *et al.* 1980) or secondary (Qian *et al.* 1996) origin, the negative excursion near the Ediacaran–Cambrian boundary observed in other regions is absent in the Meishucun section. This observation is consistent with and supportive of the conclusion made from field observations and stratigraphic analyses by Qian *et al.* (1996) that there was a depositional break between the 'Xiaowaitoushan Member' and the Zhongyicun Member in the region west of the Dianchi Fault in eastern Yunnan.

4.d.2. Pre-Tommotian positive $\delta^{13}C$ excursions

According to Brasier *et al.* (1996), the C-isotopic features D (2.0 ‰) and E (1.8 ‰) occurring in limestone of the lower Bayan Gol Formation in Mongolia compare reasonably well in position and magnitude to peak I (3.4 ‰) occurring in dolostone of the uppermost Yudoma Formation in the Aldan River area, SE Siberia, which is also supported by $^{87}Sr/^{86}Sr$ values and cross-plots of small shelly fossils. However, there is no matchable C-isotopic excursion in the Aldan River area, E Siberia, to the more positive excursion F (5.1 ‰) above E in the upper Bayan Gol Formation in Mongolia which contains the supposed Tommotian fauna.

A large positive $\delta^{13}C$ excursion (5.4 ‰) occurring in shallow-marine limestone of the Medvezhya Formation close to the Nemakit–Daldynian/Tommotian boundary at the western Anabar uplift, NW Siberia, was first discovered by Pokrovsky & Missarzhevsky (1993). Knoll *et al.* (1995*b*) and Kaufman *et al.* (1996) named this large excursion peak I′ (Fig. 7b) and argued that during the depositional interval of peaks I and I′ at the Anabar uplift of NW Siberia, only peak I appeared in the Aldan River area of SE Siberia due to a depositional hiatus between the Yudoma Formation and the overlying Pestrotsvet Formation with an apparent karstic surface in between. Consequently, radiation of small shelly fossils of the *N. sunnaginicus* Zone occurred gradually in the stratum interval between a point slightly above C-isotope peak I and a point slightly above peak I′ in NW Siberia, whereas in SE Siberia these fossils occurred together suddenly in the stratum above peak I. Kaufman *et al.* (1996) and Kouchinsky *et al.* (2001) suggested that the hiatus between the upper Yudoma Formation (Nemakit–Daldynian ± early Tommotian) and lower Pestrotsvet Formation (Tommotian) in the Aldan area lasted too long (several million years) to be considered intrazonal, and thus could be more reasonably regarded as a pre-Tommotian interval.

Recently, at the Bol'shaya Kuonamka section in the eastern Anabar uplift, which belong to an open-marine facies, three distinct positive excursions (I′, I'_a, I'_b in upward sequence) were discovered in lower beds of the Emyaksin Formation (argillaceous carbonates), and were believed to succeed peak I in SE Siberia (Kouchinsky *et al.* 2001). Of these three, I′ (∼ 5 ‰) was correlated litho- and biostratigraphically with I′ (5.4 ‰) at the western Anabar uplift, leaving the other two (I'_a, I'_b, both ∼ 3.5 ‰) no counterpart at the western Anabar uplift, probably because the eastern Anabar region was in a more offshore depositional environment than the west during the period when the early Cambrian transgression began from the north (Kouchinsky *et al.* 2001). Similarly, at the Selinde section, SE Siberia, which is near to but represents more offshore facies than transitional facies at the Dvortsy section in the Aldan River area, positive $\delta^{13}C$ oscillations (I'_n, frequent oscillations from 3 to 4.5 ‰)

https://doi.org/10.1017/S0016756809006268 Published online by Cambridge University Press

have been observed within limestones of the basal Pestrotsvet Formation, which is the uppermost level of the Nemakit–Daldynian stage. This oscillatory positive shift indicates a protracted period of minor positive values after I′ and probably embraces I'_a, I'_b of the Bol'shaya Kuonamka section at the eastern Anabar uplift (Kouchinsky *et al.* 2005). A similar positive I′-type excursion (4 ‰) has been reported from the upper Kessyusa Formation of the Olenek uplift (Knoll *et al.* 1995*a*), and a large I′-type peak (peak 6p, > 6 ‰) with a minor I'_n-type peak above (peak 7p, ~ 1.5 ‰) has also been reported from shelf carbonates of the uppermost Sukharikha Formation at Sukharikha River, western margin of Siberia (Kouchinsky *et al.* 2007).

Brasier *et al.* (1990) studied the Meishucun section and suggested correlations between the *Anabarites trisulcatus–Protohertzina anabarica* Zone (Zone I) in E Yunnan and the *Anabarites trisulcatus* Zone in E Siberia, and between the *Paragloborilus–Siphogonuchites* (Zone II) in E Yunnan and the *Purella antiqua* Zone in E Siberia. As both zones in Siberia belong to the Nemakit–Daldynian Stage, such correlations imply that Zone II in the upper Zhongyicun and Dahai Member of the Meishucun section are considered to be slightly older than the classic Tommotian fossil assemblages. At the Laolin section and the nearby Zhujiaqing section, a *Heraultipegma yunnanensis* Zone was observed by Qian *et al.* (1996, 2002) and Zhu *et al.* (2001) in the upper Dahai limestone, which was not deposited in the region west of the Dianchi Fault. There are many common fossils between the *Siphogonuchites–Paragloborilus* Zone to *Heraultipegma* Zone (the upper Zhongyicun to Dahai Member) in eastern Yunnan and the *N. sunnaginicus* Zone (top Manykai to Medvezhya Formation) in NW Siberia, such as *Halkieria sp*., *Latouchella maidipingensis*, *Latouchella korobkovi*, *Rostroconus sp*., *Igorella ungulata*, *Ovalitheca sp., Turcutheca sp*., *Bemella sp*. (Qian, 1999; Qian *et al.* 2002; Kaufman *et al.* 1996). Therefore, positive excursion L4 (3.5 ‰) which occurs in the upper Dahai Member (*Heraultipegma yunnanensis* Zone) should correlate with I′ in the top Medvezhya Formation in NW Siberia, and peaks $L2_1$ to L3 possibly correlate with peaks Z to I in NW Siberia (Knoll *et al.* 1995*b*; Kaufman *et al.* 1996) and with features A to E in Mongolia (Brasier *et al.* 1996). As mentioned above, the interval from the top Manykai Formation to the Medvezhya Formation in NW Siberia, which contains I′, is regarded as a pre-Tommotian interval, thus the upper Dahai Member which contains L4 should belong to the Pre-Tommotian Stage of the Cambrian. This further supports the correlation of the positive excursion L4 (3.5 ‰) at the Dahai Member below the Tommotian-type *Sinosachites–Tannuolina* Zone of the Shiyantou Formation with the Mongolian Feature F, which has a similar $\delta^{13}C$ magnitude (5.1 ‰) and position immediately below the Tommotian-type *Tiksitheca licis* Zone (Brasier *et al.* 1996) and also with the $\delta^{13}C$ peak (~ 4.5 ‰) occurring in phosphate-rich carbonate beds which contain maximum abundance of small shelly fossils of the basal Upper Shale Member overlain by shales having Tommotian-type fossils at the Valiabad section in northern Iran (Brasier *et al.* 1990; Kimura *et al.* 1997).

The large positive excursion (7.3 ‰) within the Dahai Member of the Xiaotan section in northeastern Yunnan (Zhou *et al.* 1997) (Fig. 6) is strikingly similar in stratigraphic position and magnitude to the positive peak (7 ‰) (Fig. 7g) in peritidal dolostones of the upper Tifnout Member belonging to the uppermost Nemakit–Daldynian parts of sections from the Anti-Atlas mountains, Morocco, where the early Cambrian strata are more expanded but lack fossils (Maloof *et al.* 2005). Correlation of the Dahai Member positive $\delta^{13}C$ excursion at the Laolin section (L4) and Xiaotan section with the Moroccan section $\delta^{13}C$ peak dated at 525.4 ± 0.5 Ma appears straightforward, which indirectly lends an age constraint for the Dahai Member.

5. Summary and concluding remarks

(1) The large negative $\delta^{13}C$ excursion observed in both this study (L1′, −7.2 ‰) and Shen & Schidlowski (2000) in the Daibu Member of the Laolin section is immediately below the FAD of small shelly fossils in the basal Zhongyicun Member of this section. The same distribution relationship between the FAD of small shelly fossils and a negative excursion of < −4 ‰ has also been observed from the Aldan River of SE Siberia (Magaritz, Holser & Kirschvink, 1986; Magaritz *et al.* 1991; Brasier *et al.* 1994) and western Anabar in NW Siberia (Pokrovsky & Missarzhevsky, 1993; Knoll *et al.* 1995*b*; Kaufman *et al.* 1996), Sukharikha River on northwestern margin of Siberia (Kouchinsky *et al.* 2007), Elburze Mountains in N Iran (Brasier *et al.* 1990; Kimura *et al.* 1997) and Mackenzie Mountains in NW Canada (Narbonne, Kaufman & Knoll, 1994). In some other regions, the FAD of small shelly fossils was found at a stratigraphic level beneath the negative excursion in Mongolia (Brasier *et al.* 1996) and at the Olenek uplift of NE Siberia (Khomentovsky & Karlova, 1993; Knoll *et al.* 1995*a*; Pelechaty *et al.* 1996; Pelechaty, Kaufman & Grotzinger, 1996). As the FADs of small shelly fossils are very likely diachronous (Brasier *et al.* 1996), and the large negative excursion may document a major biogeochemical event involving the world ocean, our data further support that the Ediacaran–Cambrian boundary is closely associated with this negative excursion. This C-isotope stratigraphic marker is particularly useful for successions where the negative C-isotope excursion occurs together with fossils having only approximate biostratigraphic significance, such as in the Turukhansk uplift on the northwestern margin of Siberia (Bartley *et al.* 1998), Nokhtuisk on the southern margin of Siberia (Pelechaty, 1998), Anti-Atlas mountains in Morocco (Magaritz *et al.* 1991;

https://doi.org/10.1017/S0016756809006268 Published online by Cambridge University Press

Maloof *et al.* 2005) and S Oman (Amthor *et al.* 2003).

(2) In contrast to the large negative excursion (L1′) in the Daibu Member beneath the Zhongyicun Member at the Laolin section, there is no clear negative excursion from the top Baiyanshao Member through the 'Xiaowaitoushan Member' to the basal Zhongyicun Member at the Meishucun section (Brasier *et al.* 1990), which lends support to the view that in the region west of the Dianchi Fault, including the Meishucun section, a depositional hiatus once occurred between the 'Xiaowaitoushan Member' (belonging to the Baiyanshao Member) and the Zhongyicun Member (Qian *et al.* 1996).

(3) The large positive excursion (L4, +3.5 ‰) found by this study in the upper Dahai Member of the Laolin section is comparable in magnitude and position not only to the succession in Xiaotan located east of the Dianchi Fault but also to the peak I′ at both eastern and western of the Anabar uplift in NW Siberia (Kaufman *et al.* 1996; Kouchinsky *et al.* 2001) and feature D in Mongolia (Brasier *et al.* 1996). All these correlative peaks are located at the biostratigraphic level of the latest Nemakit–Daldynian stage. It requires further study to determine whether there are correlated C-isotope excursions in the strata above the Dahai Member in NE Yunnan to peaks I'_a & I'_b at the eastern Anabar uplift in NW Siberia (Kouchinsky *et al.* 2001), peak I'_n at the Selinda section in E Siberia (Kouchinsky *et al.* 2005) and peak 7p at Sukharikha River, western margin of Siberia (Kouchinsky *et al.* 2007), which are suggested being above peak I′.

(4) The positive excursion (S3) assigned to the Dahai Member of the previously published C-isotope curve for the Laolin section has $\delta^{13}C$ values lower than 0 (Shen & Schidlowski, 2000), which cannot be reconciled with excursion L4 (+3.5 ‰) in Dahai Member observed in this study. The most likely explanation for this discrepancy is that this previously published C-isotope curve was incomplete and missed at least the upper Dahai limestone, as this unit was not mentioned in the lithological description given for the section by Shen & Schidlowski (2000).

In summary, this study supports the notion that the Ediacaran–Cambrian boundary is associated with a large negative $\delta^{13}C$ excursion, and that the Laolin section and the Xiaotan section in northeastern Yunnan are the best candidates for a supplementary carbonate-dominated Global Stratotype Section and Point for the Ediacaran–Cambrian boundary on the Yangtze Platform.

Acknowledgements. We thank Mao-Yan Zhu for discussion and assistance in fieldwork, and Graham Shields for his comments and English polishing. Martin Brasier and an anonymous reviewer are thanked for their constructive criticism. We also thank Ming-Yuan Lai and Tao Yang for their assistance in measuring carbon and oxygen isotope compositions, and Yu-Guan Pan for XRD analysis. This research was supported by NSFC grants 40572017, 40872025, 40232020 and 40172041 and a Doctoral Station Grant of the Education Ministry of China.

References

AMTHOR, J. E., GROTZINGER, J. P., SCHRÖDER, S., BOWRING, S. A., RAMEZANI, J., MARTIN, M. W. & MATTER, A. 2003. Extinction of *Cloudina* and *Namacalathus* at the Precambrian–Cambrian boundary in Oman. *Geology* **31**, 431–4.

BARTLEY, J. K., POPE, M., KNOLL, A. H., SEMIKHATOV, M. A. & PETROV, P. YU. 1998. A Vendian–Cambrian boundary succession from the northwestern margin of the Siberian Platform: stratigraphy, palaeontology, chemostratigraphy and correlation. *Geological Magazine* **135**, 473–94.

BATHURST, R. G. C. 1975. Carbonate sediments and their diagenesis. *Development in Sedimentology* **12**, 1–658. Amsterdam: Elsevier.

BOWRING, S. A., GROTZINGER, J. P., ISACHSEN, C. E., KNOLL, A. H., PELECHATY, S. M. & KOLOSOV, P. 1993. Calibrating rates of Early Cambrian evolution. *Science* **261**, 1293–8.

BRASIER, M. D. 1989. On mass extinctions and faunal turnover near the end of the Precambrian. In *Mass extinctions, processes, and evidence* (ed. S. K. Donovan), pp. 73–88. New York: Columbia University Press.

BRASIER, M. D., COWIE, J. & TAYLOR, M. 1994. Decision on the Precambrian–Cambrian boundary stratotype. *Episodes* **17**, 3–8.

BRASIER, M. D., MAGARITZ, M., CORFIELD, R., LUO, H.-L., WU, X.-C., OUYANG, L., JIANG, Z.-W., HAMDI, B., HE, T.-G. & FRASER, A. G. 1990. The carbon- and oxygen-isotope record of the Precambrian–Cambrian boundary interval in China and Iran and their correlation. *Geological Magazine* **127**, 319–32.

BRASIER, M. D., ROZANOV, A. YU., ZHURAVLEV, A. YU., CORFIELD, R. M. & DERRY, L. A. 1994. A carbon isotope reference scale for the Lower Cambrian succession in Siberia: report of IGCP Project 303. *Geological Magazine* **131**, 767–83.

BRASIER, M. D., SHIELDS, G., KULESHOV, V. N. & ZHEGALLO, E. A. 1996. Integrated chemo- and biostratigraphic calibration of early animal evolution: Neoproterozoic–early Cambrian of southwest Mongolia. *Geological Magazine* **133**, 445–85.

COWIE, J. W. 1985. Continuing work on the Precambrian–Cambrian boundary. *Episodes* **8**, 93–7.

CRAIG, H. 1953. The geochemistry of stable carbon isotopes. *Geochimica et Cosmochimica Acta* **3**, 53–92.

GEYER, G. & UCHMAN, A. 1995. Ichnofossil assemblages from the Nama Group (Neoproterozoic–lower Cambrian) in Namibia and the Proterozoic–Cambrian boundary problem revisited. *Beringeria Special Issue* **2**, 175–202.

GROTZINGER, J. P., BOWRING, S. A., SAYLOR, B. Z. & KAUFMAN, A. J. 1995. Biostratigraphic and geochronologic constraints on early animal evolution. *Science* **270**, 598–604.

HE, T.-G. 1989. Classification and correlation of phosphatic sequences of Yuhucun Formation in east Yunnan. *Minerals and Rocks* **9**(2), 1–11 (in Chinese with English abstract).

HE, T.-G., SHEN, L.-J. & YIN, J.-C. 1988. A new understanding on Meishucun Sinian–Cambrian boundary

section in Jinning, Yunnan. *Journal of Chengdu College of Geology* **15**(3), 38–44 (in Chinese with English abstract).

JIANG, Z.-W. 1980. The Meishucun Stage and fauna of the Jinning County, Yunnan. *Bulletin of the Chinese Academy of Geological Sciences* **2**(1), 75–96 (in Chinese with English abstract).

KAUFMAN, A. J. & KNOLL, A. H. 1995. Neoproterozoic variations in the C-isotopic composition of seawater: stratigraphic and biogeochemical implications. *Precambrian Research* **73**, 27–49.

KAUFMAN, A. J., KNOLL, A. H., SEMIKHATOV, M. A., GROTZINGER, J. P., JACOBSEN, S. B. & ADAMS, W. 1996. Integrated chronostratigraphy of Proterozoic–Cambrian boundary beds in the western Anabar region, northern Siberia. *Geological Magazine* **133**, 509–33.

KHOMENTOVSKY, V. V. & KARLOVA, G. A. 1993. Biostratigraphy of the Vendian–Cambrian beds and the Lower Cambrian boundary in Siberia. *Geological Magazine* **130**, 29–45.

KIMURA, H., MATSUMOTO, R., KAKUWA, Y., HAMDI, B. & ZIBASERESHT, H. 1997. The Vendian–Cambrian $\delta^{13}C$ record, North Iran: evidence for overturning of the ocean before the Cambrian Explosion. *Earth and Planetary Science Letters* **147**, E1–E7.

KIMURA, H. & WATANABE, Y. 2001. Oceanic anoxia at the Precambrian–Cambrian boundary. *Geology* **29**, 995–8.

KNOLL, A. H. & CARROLL, S. B. 1999. Early animal evolution: Emerging views from comparative biology and geology. *Science* **284**, 2129–37.

KNOLL, A. H., GROTZINGER, J. P., KAUFMAN, A. J. & KOLOSOV, P. 1995*a*. Integrated approaches to terminal Proterozoic stratigraphy: An example from the Olenek Uplift, northeastern Siberia. *Precambrian Research* **73**, 251–70.

KNOLL, A. H., KAUFMAN, A. J., SEMIKHATOV, M. A., GROTZINGER, J. P. & ADAMS, W. 1995*b*. Sizing up the sub-Tommotian unconformity in Siberia. *Geology* **23**, 1139–43.

KOUCHINSKY, A., BENGTSON, S., MISSARZHEVSKY, V. V., PELECHATY, S., TOSSANDER, P. & VAL'KOV, A. K. 2001. Carbon isotope stratigraphy and the problem of a pre-Tommotian Stage in Siberia. *Geological Magazine* **138**, 387–96.

KOUCHINSKY, A., BENGTSON, S., PAVLOV, V., RUNNEGAR, B., TORSSANDER, P., YOUNG, E. & ZIEGLER, K. 2007. Carbon isotope stratigraphy of the Precambrian–Cambrian Sukharikha River section, northwestern Siberian platform. *Geological Magazine* **144**, 609–18.

KOUCHINSKY, A., BENGTSON, S., PAVLOV, V., RUNNEGAR, B., VAL'KOV, A. & YOUNG, E. 2005. Pre-Tommotian age of the lower Pestrotsvet Formation in the Selinde section on the Siberian platform: carbon isotopic evidence. *Geological Magazine* **142**, 319–25.

KUMP, L. R. 1991. Interpreting carbon-isotope excursions: Strangelove oceans. *Geology* **19**, 299–302.

LANDING, E. 1994. Precambrian–Cambrian boundary global stratotype ratified and a new perspective of Cambrian time. *Geology* **22**, 179–82.

LARSON, A. C. & VON DREELE, R. B. 2004. *General Structure Analysis System (GSAS), Los Alamos National Laboratory Report LAUR*, pp. 86–748.

LATHAM, A. & RIDING, R. 1990. Fossil evidence for the location of the Precambrian/Cambrian boundary in Morocco. *Nature* **344**, 752–4.

LUO, H.-L., JIANG, Z.-W. & TANG, L.-D. 1994. *Stratotype section for Lower Cambrian stages in China*. Kunming: Yunnan Science and Technology Press (in Chinese with English summary), pp. 1–183 + 40 pp.

LUO, H.-L., JIANG, Z.-W., WU, X.-C., SONG, X.-L. & OUYANG, L. 1982. *The Sinian–Cambrian boundary in eastern Yunnan, China*, pp. 1–265. Kunming: People's Publishing House, Yunnan (in Chinese with English summary).

LUO, H.-L., JIANG, Z.-W., WU, X.-C., SONG, X.-L. & OUYANG, L. 1990. The global biostratigraphical correlation of the Meishucunian stage and the Precambrian–Cambrian boundary. *Science in China (Series B)* **14**(3), 313–18 (in Chinese).

LUO, H.-L., JIANG, Z.-W., WU, X.-C., SONG, X.-L., OUYANG, L., XING, Y.-S., LIU, G.-Z., ZHANG, S.-S. & TAO, Y.-H. 1984. *Sinian–Cambrian boundary stratotype section at Meishucun, Jinning, China*, pp. 1–154. Kunming: People's Publishing House, Yunnan (in Chinese with English summary).

LUO, H.-L., JIANG, Z.-W., XU, Z.-J., SONG, X.-L. & XUE, X.-F. 1980. On the Sinian–Cambrian boundary of Meichcun and Wangjiawan, Jinning County, Yunnan. *Acta Geologica Sinica* **1980**(2), 95–112 (in Chinese with English abstract).

LUO, H.-L., WU, X.-C. & OUYANG, L. 1991. Facies changes and transverse correlation of the Sinian–Cambrian boundary strata in eastern Yunnan. *Sedimentary Facies and Palaeogeography* **1991**(4), 27–35 (in Chinese with English abstract).

MAGARITZ, M., HOLSER, W. T. & KIRSCHVINK, J. L. 1986. Carbon-isotope events across the Precambrian/Cambrian boundary on the Siberian Platform. *Nature* **320**, 258–9.

MAGARITZ, M., KIRSCHVINK, J. L., LATHAM, A. J., ZHURAVLEV, A. YU. & ROZANOV, A. YU. 1991. Precambrian/Cambrian boundary problem: Carbon isotope correlations for Vendian and Tommotian time between Siberia and Morocco. *Geology* **19**, 847–50.

MALOOF, A. C., SCHRAG, D. P., CROWLEY, J. L. & BOWRING, S. A. 2005. An expanded record of Early Cambrian carbon cycling from the Anti-Atlas Margin, Morocco. *Canadian Journal of Earth Sciences* **42**, 2195–216.

MCCREA, J. M. 1950. On the isotopic chemistry of carbonates and a paleotemperature scale. *The Journal of Chemical Physics* **18**, 849–57.

NARBONNE, G. M., KAUFMAN, A. J. & KNOLL, A. H. 1994. Integrated chemostratigraphy and biostratigraphy of the Windermere Supergroup, northwestern Canada: Implications for Neoproterozoic correlations and the early evolution of animals. *Geological Society of America Bulletin* **106**, 1281–92.

NARBONNE, G. M., MYROW, P. M., LANDING, E. & ANDERSON, M. M. 1987. A candidate stratotype for the Precambrian–Cambrian boundary, Fortune Head, Burin Peninsula, southeastern Newfoundland. *Canadian Journal of Earth Sciences* **24**(7), 1277–93.

PELECHATY, S. M. 1998. Integrated chronostratigraphy of the Vendian System of Siberia: implications for a global stratigraphy. *Journal of the Geological Society, London* **155**, 957–73.

PELECHATY, S. M., GROTZINGER, J. P., KASHIRTSEV, V. A. & ZHERNOVSKY, V. P. 1996. Chemostratigraphic and sequence stratigraphic constraints on Vendian–Cambrian basin dynamics, Northeast Siberian Craton. *Journal of Geology* **104**, 543–63.

PELECHATY, S. M., KAUFMAN, A. J. & GROTZINGER, J. P. 1996. Evaluation of $\delta^{13}C$ chemostratigraphy for intrabasinal correlation: Vendian strata of northeast

Siberia. *Geological Society of America Bulletin* **108**, 992–1003.

POKROVSKY, B. G. & MISSARZHEVSKY, V. V. 1993. Izotopnaya korrelyatsiya pogranichnykh tolsch dokembriya i kembriya Sibirskoj platformy. [Isotopic correlation of Precambrian and Cambrian boundary beds of the Siberian platform.] *Doklady Akademii Nauk* **329**, 768–71 (in Russian).

QIAN, Y. 1977. Hyolitha and some Problematica from the Lower Cambrian Meishucun Stage in central and southwest China. *Acta Palaeontologica Sinica* **16**(2), 255–78 (in Chinese with English abstract).

QIAN, Y. 1999. *Taxonomy and biostratigraphy of small shelly fossils in China*. Beijing: Science Press (in Chinese), 78 pp.

QIAN, Y. & BENGTSON, S. 1989. Palaeontology and biostratigraphy of the Early Cambrian Meishucunian Stage in Yunnan Province, South China. *Fossils and Strata* **24**, 1–156.

QIAN, Y., ZHU, M.-Y., HE, T.-G. & JIANG, Z.-W. 1996. New investigation of Precambrian–Cambrian boundary sections in eastern Yunnan. *Acta Micropalaeontologica Sinica* **13**(3), 225–40 (in Chinese with English abstract).

QIAN, Y., ZHU, M.-Y., LI, G.-X., JIANG, Z.-W. & ITEN, H. V. 2002. A supplemental Precambrian–Cambrian boundary global stratotype section in SW China. *Acta Palaeontologica Sinica* **41**(1), 19–26.

ROSENBAUM, J. & SHEPPARD, S. M. F. 1986. An isotopic study of siderites, dolomites and ankerites at high temperatures. *Geochimica et Cosmochimica Acta* **50**, 1147–50.

SEILACHER, A. 1984. Late Precambrian and Early Cambrian metazoa: Preservational or real extinctions? In *Patterns of change in Earth evolution* (eds H. D. Holland & A. F. Trendall), pp. 159–68. Berlin: Springer-Verlag.

SHEN, Y.-A. & SCHIDLOWSKI, M. 2000. New C isotope stratigraphy from southwest China: Implications for the placement of the Precambrian–Cambrian boundary on the Yangtze Platform and global correlations. *Geology* **28**, 623–6.

SHEN, Y.-A. & SCHIDLOWSKI, M. 2001. New C isotope stratigraphy from southwest China: Implications for the placement of the Precambrian–Cambrian boundary on the Yangtze Platform and global correlations: reply. *Geology* **29**, 872.

SHIELDS, G. 1999. Working towards a new stratigraphic calibration scheme for the Neoproterozoic–Cambrian. *Eclogae Geologicae Helvetiae* **92**(2), 221–33.

STRAUSS, H., DE MARAIS, D. J., HAYES, J. M. & SUMMONS, R. E. 1992. The carbon isotopic record. In *The Proterozoic Biosphere* (eds J. W. Schopf & C. Klein), pp. 117–27. Cambridge: Cambridge University Press.

TUCKER, M. E. 1986. Carbon isotope excursions in Precambrian/Cambrian boundary beds, Morocco. *Nature* **319**, 48–50.

XING, Y.-S., DING, Q.-X., LUO, H.-L., HE, T.-G. & WANG, Y.-G. 1984. The Sinian–Cambrian boundary of China and its related problems. *Geological Magazine* **121**, 155–70.

YIN, J.-C., LI, D.-Q. & HE, T.-G. 1993. New discovery of trace fossils from the Sinian–Cambrian beds in eastern Yunnnan and its significance for global correlation. *Acta Geologica Sinica* **67**(2), 146–58 (in Chinese with English abstract).

ZHOU, C.-M., ZHANG, J.-M., LI, G.-X. & YU, Z.-Y. 1997. Carbon and oxygen isotopic record of the early Cambrian from the Xiaotan section, Yunnan, South China. *Scientia geologica sinica* **32**(2), 201–11 (in Chinese with English abstract).

ZHU, M.-Y., LI, G.-X. & ZHANG, J.-M. 2001. New C isotope stratigraphy from southwest China: Implications for the placement of the Precambrian–Cambrian boundary on the Yangtze Platform and global correlations: Comment. *Geology* **29**, 871.

ZHU, M.-Y., LI, G.-X., ZHANG, J.-M., STEINER, M., QIAN, Y. & JIANG, Z.-W. 2001. Early Cambrian stratigraphy of east Yunnan, southwestern China: A synthesis. *Acta Palaeontologica Sinica* **40**(Supplement), 4–39.

ZHU, M.-Y., ZHANG, J.-M., STEINER, M., YANG, A.-H., LI, G.-X. & ERDTMANN, B. D. 2003. Sinian–Cambrian stratigraphic framework for shallow- to deep-water environments of the Yangtze Platform: an integrated approach. *Progress in Natural Science* **13**, 951–60.